Available online at www.sciencedirect.com
SCIENCE DIRECT
Coordination Chemistry Reviews 250 (2006) 212–241
COORDINATION CHEMISTRY REVIEWS
www.elsevier.com/locate/ccr

Review

Metallocene catalyzed ethene- and propene co-norbornene polymerization: Mechanisms from a detailed microstructural analysis

Incoronata Tritto *, Laura Boggioni, Dino R. Ferro

Istituto per lo Studio delle Macromolecole, Consiglio Nazionale delle Ricerche, Via E. Bassini 15, I-20133 Milano, Italy

Received 8 February 2005; accepted 22 June 2005
Available online 2 September 2005

Contents

* Corresponding author. Tel.: +39 0223699370; fax: +39 0270636400.
E-mail addresses: i.tritto@ismac.cnr.it (I. Tritto), boggioni@ismac.cnr.it (L. Boggioni), ferro@ismac.cnr.it (D.R. Ferro).

doi:10.1016/j.ccr.2005.06.019

Abstract

Cyclic olefin copolymers are one of the new families of olefinic copolymers made available by metallocenes. Owing to their unique combination of properties, they are engineered polymers which are produced and commercialized. This review provides an overview of recent progress regarding ethene (E)– and propene (P)–norbornene (N) copolymerization with early transition metal catalysts. Metallocenes and some of post metallocene catalyst precursors most frequently utilized for the synthesis of norbornene copolymers are presented.
The synthesis and the experimental studies which provided our current knowledge of factors governing copolymerization activity, copolymer tacticity, and molar mass are reviewed. In particular, we focus on the elucidation of E–N and P–N copolymer microstructure through ^{13}C NMR analysis. Advances in signal assignments of the complex spectra of these copolymers are reviewed together with various methodologies utilized to achieve them. The microstructural description of the E–N chain, attained from such assignments, is summarized along with information achieved on the copolymerization mechanisms. The detailed information on the microstructure of these copolymers at tetrad or at pentad level has been applied to determine the kinetic copolymerization parameters and shed light on the polymerization mechanisms. Finally, a few relevant topics which contribute to our understanding of the mechanisms of initiation, propagation, termination, and chain-transfer steps are presented. These include a few examples of modern density functional calculations, chain end groups analysis, and synthesis of hydro-oligomers.

Keywords: Norbornene copolymerization; Metallocene catalysts; Copolymer microstructure; ^{13}C NMR analysis; Statistical models; Polymerization mechanisms

1. Introduction

The discovery and the development of well defined metallocene catalysts [1] have opened great opportunities for the synthesis of a wide range of polymers with selected architectures. Catalysts are now available for unprecedented control of poly-α-olefin stereospecificity and properties and for the synthesis of new polyolefin families [1]. By using such catalysts, the cyclic olefin polymers can be synthesized via addition polymerization without ring-opening metathesis in contrast to the behavior of conventional heterogeneous Ziegler–Natta catalysts [2]. Cyclic olefin monomers that can be polymerized using metallocene catalysts via addition are shown in Chart 1: they include cyclopentene, cyclobutene, and norbornene [3]. They provide a new class of polymeric materials with interesting properties. Scheme 1 illustrates the two alternative polymerizations of cyclic olefins: via ring opening metathesis (ROMP) and via addition.

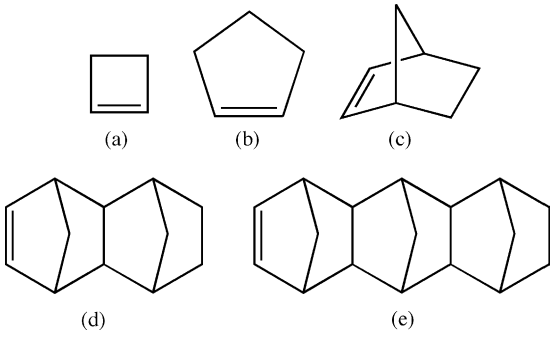

Chart 1. Cyclic olefins that are polymerized by metallocene catalysts via addition: (a) cyclobutene; (b) cyclopentene; (c) norbornene; (d) 1,4,5,8-dimethano-1,2,3,4,4a,5,8,8a-octahydronaphtalene (DMON); (e) 1,4,5,8,9,10-trimethano1,2,3,4,4a,5,8,8a,9,9a,10,10a-dodecahydroantracene (TMDA).

The overall ROMP reaction involves breaking and reforming olefin double bonds with simultaneous opening of the unsaturated cycles of the monomers [4]. The release of ring strain [5] provides the main driving force required to overcome the unfavorable entropy change in polymerisation [6,7]. Accordingly, low-strained cyclohexene is difficult to polymerize [8], while norbornene having a ring strain of more than 15 kcal/mol undergoes reaction readily with a large number of metathesis catalysts [9].

On the other hand, the reactivity of cycloolefin in addition polymerization is strongly influenced by the ring strain of the cyclic olefin as well as by the non-planarity of the reacting double bond, which can be described by symmetric or antisymmetric deformation (cycloolefins with symmetric out-of-plane such as norbornene and cyclopentene can be polymerized; cycloolefins with antisymmetric out-of-plane

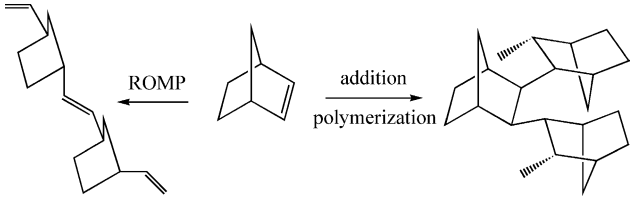

Scheme 1. The two alternative polymerizations of cyclic olefins: via ring opening metathesis (ROMP) and via addition.

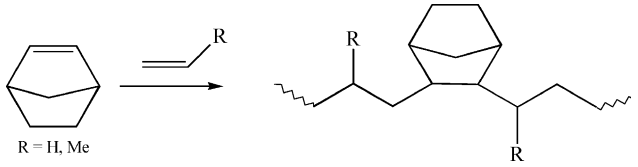

Fig. 1. COCs considered in this review: E–N copolymers (R = H) and P–N copolymers (R = Me).

bending such as cyclooctene cannot be homopolymerized). Moreover, the possibility of monocyclic monomers like cyclopentene of undergoing β-hydrogen elimination, which leads to isomerization and termination of the growing polymer chain has consequences for the polymer structure and polymer molar mass [10].

Saturated cycloaliphatic polymers, having high decomposition temperatures, small optical birefringence, good transparency for short wavelength radiation and high plasma etch resistance, are suitable for advanced photoresist composition in the microelectronic industry [11]. Such polymers can be obtained for example by palladium, nickel, and cobalt catalysts [12]. However, cycloolefin homopolymers by metallocenes are not processable due to their low solubility in organic solvents and their melting points are higher than the decomposition temperature [3].

Among the new polymer families, *ansa*-metallocene catalysts enable the synthesis of cyclic olefin copolymers (COCs) with various comonomer content and microstructures. Among them the most versatile and interesting ones are the ethene (E)–norbornene (N) copolymers (Fig. 1, R = H).

They were first synthesized by Kaminsky et al. with *ansa*-zirconocenes in 1991 [3]. Since then, both academic and industrial groups have focused their research interest on COCs. Ticona (formerly Hoechst) and Mitsui have developed these copolymers to commercial products TOPAS [13] and APEL [14], respectively. E–N copolymers are usually amorphous and display a wide range of glass transition temperatures, from room temperature to about 220 °C. They show excellent transparency and high refractive index because of their rigid bicyclic monomer units, high chemical resistance, and good processability [15]. These properties, imparted by the norbornene component, make COCs suitable for optical applications such as coatings for high-capacity CDs and DVDs, for lenses, medical equipments, blisters, toner binder, and packaging.

In this review, we summarize recent progress regarding norbornene copolymerization via addition. An overview of the early transition metal catalysts used for the synthesis of norbornene copolymers will be given. In Chart 2 the structures of some of the metallocenes most frequently used for olefin-norbornene copolymerizations are presented. Of course metallocenes are catalyst precursors, which need to be activated by cocatalysts, the most widely used being methylaluminoxane (MAO).

In particular we focus on the synthesis of ethene- and propene co-norbornene polymers catalyzed by metallocenes and on the elucidation of their microstructure through ^{13}C NMR analysis. With respect to norbornene homopolymers prepared in the presence of the same catalysts, the copolymers have the great advantage of being processable. Their properties depend on many parameters, such as the comonomer composition, the distribution of comonomers within the chain, and also the chain stereoregularity, which are determined by the structure of the catalyst precursor. The design of norbornene based materials with given features requires a detailed description of the microstructure of copolymers as well as a deep understanding of the relationships between the microstructure and the material properties. Although the first synthesis of E–N copolymers was reported as early as 1991 [3], their microstructure has only recently been thoroughly investigated.

^{13}C NMR spectroscopy is surely the most powerful analytical tool for polymer microstructural investigation. However, E–N copolymer spectra are quite complex for the presence in the polymer chain of two stereogenic carbons per norbornene unit and for the fact that the chemical shifts of these copolymers do not obey straightforward additive rules, owing to the bicyclic nature of the norbornene structural units. Thus, until recently analyses of ^{13}C NMR spectra were scarce and the calculation of N mol% in the copolymers was only straightforward in the case of copolymers with not too high N content.

A description of these copolymers as well as a detailed understanding of the processes and mechanisms involved in these copolymerizations proved difficult to be achieved. Only in the last few years have a number of groups accepted the challenge of assigning the ^{13}C NMR spectra of E–N copolymers. Advances in signal assignments will be reviewed together with various methodologies utilized to achieve them.

We shall discuss how the detailed information on the E–N chain microstructure has been applied to determine the kinetic copolymerization parameters and shed light on the polymerization mechanisms.

Recently, there has been also intense interest in synthesizing E–N copolymers with a variety of late transition metal catalysts, namely nickel and palladium based catalysts, which are tolerant towards polar groups. Late transition metal catalyzed ethene cycloolefin copolymerization will not be covered by this review, however a list of relevant papers is included [16].

2. Ethene–norbornene copolymers

2.1. Structure

Early studies showed that norbornene in metallocene catalyzed copolymerization is enchained by *cis*-2,3-exo addition [3]. A segment of an E–N copolymer (EENEE) in which norbornene can be considered isolated from other norbornene units is shown in Fig. 2 along with the adopted numbering of carbon atoms. Fig. 3 gives an overview of possible segments

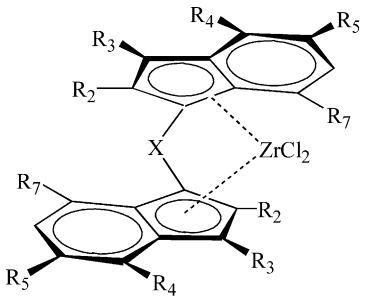

I

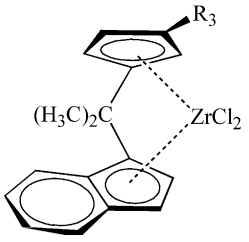

II

X = CH_2-CH_2,	all R = H, indenyl = indenylH_4	(**I-1**)
	all R = H	(**I-2**)
	$R_4 = R_7 = CH_3$	(**I-3**)
X = $(CH_3)_2Si$,	all R = H	(**I-4**)
	R_4 - R_5= benz	(**I-5**)
	$R_2 = CH_3$, R_4 - R_5= benz	(**I-6**)
	$R_2 = CH_3$	(**I-7**)
X = $(CH_3)_2C$,	all R = H	(**I-8**)
X = CH_2	R_3 = ^{t}Bu	(**I-9**)
X = $(Ph)_2Si$,	all R = H	(**I-10**)

(only R ≠ H are indicated)

R_3 = H	(**II-1**)
R_3 = ^{i}Pr	(**II-2**)

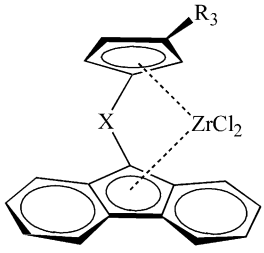

III

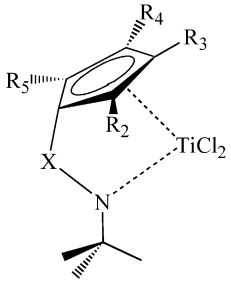

IV

X = $(CH_3)_2C$,	R_3 = H	(**III-1**)	X = Me_2Si,	$R_2 = R_3 = R_4 = R_5 = CH_3$	(**IV-1**)
	$R_3 = CH_3$	(**III-2**)		$R_3 = R_5 = CH_3$	(**IV-2**)
	R_3 = ^{i}Pr	(**III-3**)		R_4 = ^{t}Bu	(**IV-3**)
	R_3 = ^{t}Bu	(**III-4**)		R_4 - R_5 = benz	(**IV-4**)
X = $(CH_3)_2Si$,	R_3 = H	(**III-5**)		R_4 - R_5 = benz, R_2 - R_3 = benz,	(**IV-5**)
X = $(Ph)_2C$,	R_3 = H	(**III-6**)	(only R ≠ H are indicated)		

Chart 2. Structures of the most frequently used metallocenes for olefin-norbornene copolymerizations.

of an E–N copolymer chain in which norbornene units are in alternating (ENENE), diad (ENNE) and triad (ENNNE) sequences, without considering stereochemical differences. The adopted numbering of norbornene carbons, which is similar to that of other authors [17], has been chosen in order to indicate differences in assignments; thus, C2, C1, and C6 are always closer to another norbornene unit than atoms C3, C4, and C5, respectively.

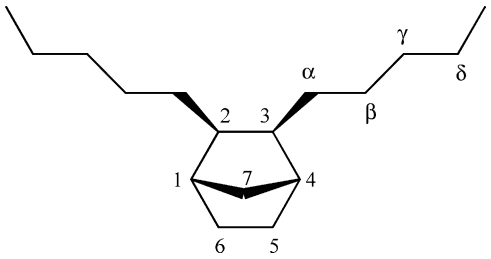

Fig. 2. A segment of E–N copolymer chain (EENEE) with isolated norbornene unit, showing the numbering of carbon atoms.

Besides the different comonomer sequences, we note that configuration at atoms C2/C3 in a ring can be either S/R or R/S, so the relationship between two subsequent norbornene units can be either erythrodiisotactic (*meso*) or erythrodisyndiotactic (*racemic*). The possible stereochemical environments of norbornene in alternating sequences, diads and triads are illustrated in Fig. 4. Erythrodiisotactic and erythrodisyndiotactic microstructures of ENENE and ENNE segments can be obtained depending on the catalyst structure [18].

2.2. Methodologies for signal assignments

The ^{13}C NMR spectrum of an E–N copolymer with 50.8 mol% of norbornene produced by catalyst *rac*-Et

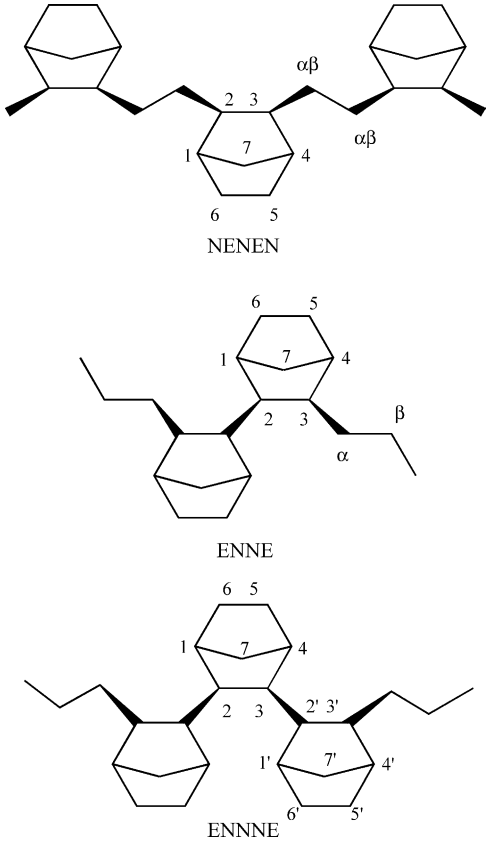

Fig. 3. Segments of E–N copolymer chain with norbornene in alternating (NENEN), diad (ENNE) and triad (ENNNE) sequences, with the adopted numbering.

$(Indenyl)_2ZrCl_2$ (**I-2**) is shown in Fig. 5. General assignments of norbornene and ethene carbons allow us to divide the simpler spectra into four regions and thus to calculate the mol% of norbornene incorporated in the polymer [17,26]. At a higher level of norbornene the spectra are more complex and the four regions may overlap, since the various stereosequences of triads and longer norbornene sequences cause splitting and shift of the signals, which can make even the norbornene content uncertain.

2.2.1. Model compounds

In principle, the synthesis of model compounds of a copolymer sequence offers the best approach to make certain assignments of the signals of the sequence and thus to successfully determine the copolymer structure and tacticity. The synthesis of model compounds is often very time consuming and not always available. The hydro-oligomerization followed by isolation of hydroisomers can be used to investigate the structure and the tacticity of the isomers, which can be considered as model compounds of a segment of the copolymer chain. However, the higher the oligomerization number, the higher is the number of possible stereoisomers and the more tedious and difficult the separation process. Arndt was able to isolate and assign the signals of all the possible norbornene hydrodimers and hydrotrimers by means of hydro-oligomerization with *ansa*-metallocenes having different symmetries [19]. These assignments have been very important, although the results of molecular mechanics show that dimers and trimers are poor models of polynorbornene and of its higher oligomers, due to strong steric interactions between non-adjacent units, which induce large deformations of the torsional angles and of the ring geometry. Yet the differences between dimers and trimers were used to understand the shifts [17,20,19]. Very recently Fink and co-workers synthesized, isolated, and characterized hydro-oligomers from dimers to pentamers of norbornene by **I-8**/MAO [21]. They found a new type of linkage in the tetramers and pentamers, similar to one found by Arndt and Gosmann [22] in a hydropentamer synthesized with **I-1**/MAO and characterized by means of X-ray.

2.2.2. NMR pulse sequences

A first general assignment of methylene (C7) and methine (C1/C4 and C2/C3) carbon atoms was achieved with the help of distortionless enhancement by polarization transfer (DEPT) ^{13}C spectra. DEPT experiments allow one to distinguish between methyl or methine and methylene carbons: the methine and methyl signals appear positive, while the methylene ones are negative. This method does not allow us to distinguish between ethene CH_2 and C5/C6 methylene carbons of norbornene in the region between 26 and 31 ppm.

2D NMR techniques and INADEQUATE ^{13}C–^{13}C correlated NMR spectra were of great help to attribute resonances of norbornene diads and in correcting previous assignments of ethene and norbornene methylenes. Bergström et al. by using ^{13}C–^{1}H correlations, hmqc for one-bond correlations, and hmbc for two- or three-bond correlations were able to identify C5/C6 and C2/C3 of norbornene diads [23].

2.2.3. Series of copolymers with different norbornene content

The comparison of spectra of copolymers with different norbornene content, obtained by catalysts with different symmetries, has helped to assign a number of resonances. However, use of this method alone is rather limited in the case of E–N copolymer spectra.

2.2.4. ^{13}C enrichment

^{13}C NMR investigations based on comparison between E–N copolymers of monomers with natural abundance of ^{13}C and those obtained with $^{13}C_1$-enriched ethene or $^{13}C_{5/6}$-enriched norbornene allowed Fink to determine the number of C5/C6 or ethene signals and to make significant advances in their assignments [24].

2.2.5. Chemical shift prediction

Theoretical methods were also of help in the interpretation of the E–N copolymer spectra and in clarifying their microstructure. Independent and complementary support to the chemical shift assignments can be achieved by interpreting NMR spectra of polymers in terms of chain conformation.

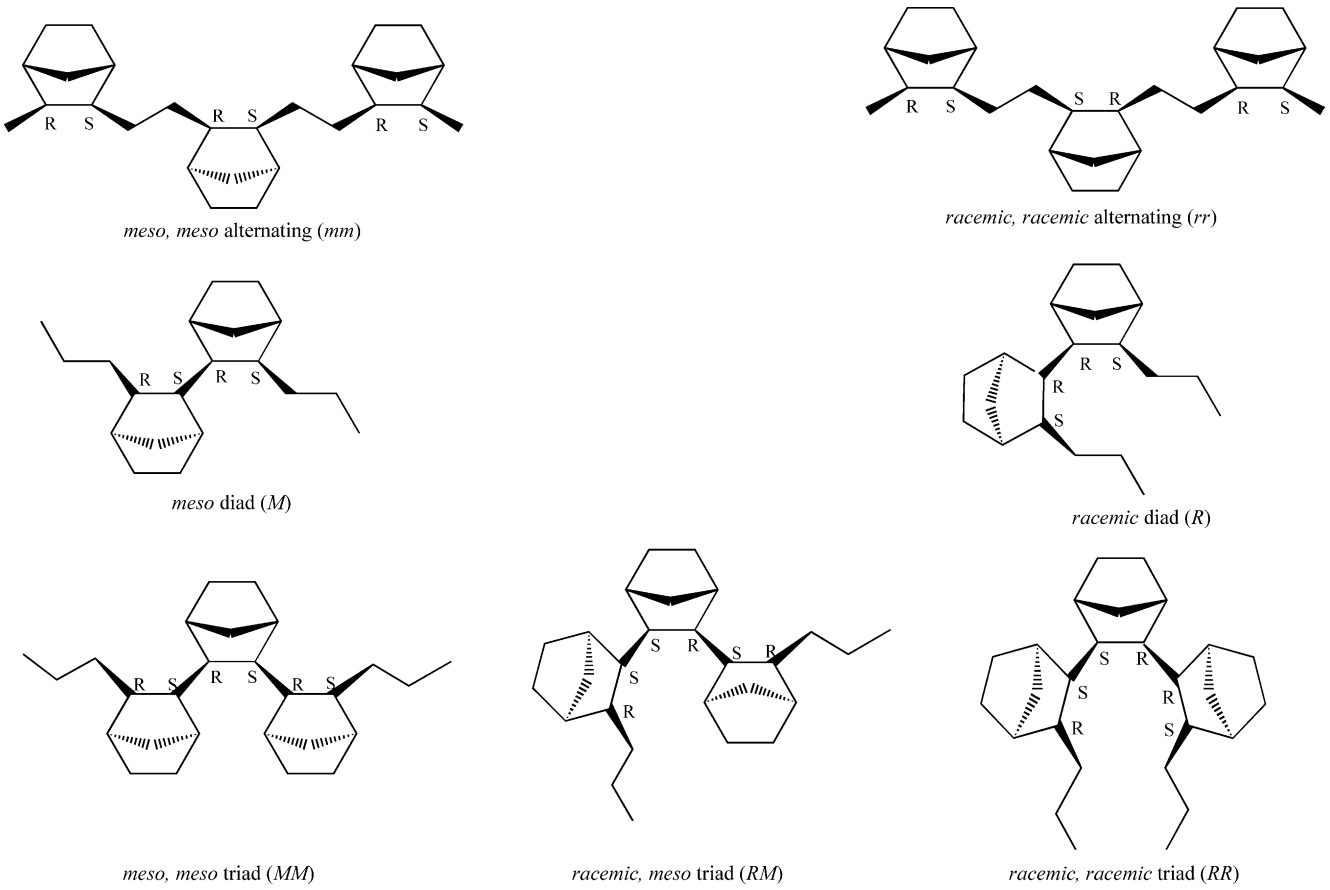

Fig. 4. Alternating (NENEN), diad (ENNE) and triad (ENNNE) sequences, showing the possible configurations.

The approach is based on determining the stable conformers by means of molecular mechanics and on considering such conformation-dependent effects as the well-known γ-gauche effect [25]. Indeed, the results obtained with a RIS model of the E–N copolymers [18] suggested for the first time and proved the occurrence of the splitting of the signals of *meso* and *racemic* alternating NEN sequences.

2.2.6. Least-squares fitting of peak areas

Extension of the assignment of unknown signals of ^{13}C NMR spectra of E–N copolymers can be obtained by trial-and-error through an analysis of the spectra based on a procedure devised for computing the molar fractions of the stereosequences that define the microstructure of an E–N copolymer [26]. An appropriate partitioning of the molecular chain into fragments, defined according to the assignment level available, is necessary. The molar fractions of such fragments represent one way for describing the chain microstructure: the observed peak areas of the greatest possible number of ^{13}C NMR signals assignable (on the basis of a list of known chemical shifts, such as Table 1 in Ref. [26], and of additional hypotheses) are utilized in a computer program [26] to generate and solve a set of linear equations where the molar fractions are the variables.

The various types of chain fragments (isolated, alternating and blocks) defined in the calculation, which also distinguishes between *meso* (*m*) and *racemic* (*r*) alternating units and between *meso* (M) and *racemic* (R) ENNE sequences, are illustrated in Ref. [26].

2.2.7. Ab initio chemical shift computations

More recently, we found that advanced quantum-mechanical methods for computing ^{13}C NMR magnetic shielding [27–29] may be applied successfully to reproduce stereo-chemical shifts of proper model compounds containing the norbornene moiety. These methods are particularly useful to evaluate the effects of molecular arrangements for which no empirical data are available, as in the case of the distortions of the N ring. Thus, GIAO/DFT calculations [27] utilizing the functional MPW1PW91 proposed by Barone and Adamo [30] confirmed independently our most recent assignments [26] related to ENNE sequences of E–N copolymers.

2.3. Alternating E–N copolymers

2.3.1. Synthesis and assignments

The synthesis of perfectly ordered sequences in copolymers is still a challenge in polymerization catalysis; however

Table 1
Alternating E–N copolymerization: activities and properties

Symmetry	Catalyst	Activity (kg pol/mol Mt h)	[N]/[E]	N mol% incorporated	T_g (T_m) (°C)	M_w ($\times 10^{-4}$ g/mol)	M_w/M_n	Ref.
C_s	**IV-1**	21000[a]	0.4	12	35	16.4		[32]
		33912[a]	1.0	22	–	34.1	–	[32]
		15960[a]	2.5	30	60	119.0	–	[32]
		11997[a]	6.8	40	94	86.2	–	[32]
	IV-2	4694[a]	2.0	34	67	40.1	–	[32]
	IV-3	520[a]	11.0	35	71	25.3	–	[32]
	IV-4	1399[a]	2.5	34	83	39.6	–	[32]
	VI-1	2730[b]	5.6	44	120	59.28	1.16	[34]
	VI-2	2154[b]	5.6	–	121	51.71	1.24	[34]
	VI-3	3186[b]	5.6	–	126	73.80	1.23	[34]
C_1	**VIII-1**	1720[c]	9	44	121	39.78	1.17	[35]
	VIII-2	580[c]	9	46	125	22.61	1.19	[35]
	VIII-3	440[c]	9	35	123	22.50	1.50	[35]
	VIII-4	3200[c]	9	48	135	87.78	1.54	[35]
	III-2	1602[d]	15.6	46	118 (243)	43.1	–	[38]
	III-3	5600[e]	9.1	42	101	–	–	[39]
	III-4	142[d]	13.3	39	103 (255)	0.89	–	[38]
C_2	**I-6**	30[f]	26.0	47	122	60.00	1.17	[51]
C_1	**VII-1**	850[g]	21	26.2	44.8	20.44	1.4	[37]
	VII-2	3510[g]	21	39.7	87.3	15.33	2.1	[37]
	VII-3	176[g]	10	27.5	54.8	2.46	4.1	[37]

[a] Polymerization condition: MAO/Ti = 2000, [Ti] = 2×10^{-5} mol/L; P_E = 0.9–4.9 bar, T = 40 °C.
[b] Polymerization condition: MAO/Ti = 1250, [Ti] = 4×10^{-6} mol/L; P_E = 1.013 bar, T = 25°C.
[c] Polymerization condition: MAO/Ti = 2000, [Ti] = 3×10^{-5} mol/L; P_E = 1.013 bar, T = 25 °C.
[d] Polymerization condition: MAO/Zr = 8620, [Zr] = 5×10^{-6} mol/L; P_E = 2.026 bar, T = 30 °C.
[e] Polymerization condition: MAO/Zr = 2200, [Zr] = 3.5×10^{-5} mol/L; P_E = 2 bar, T = 20 °C.
[f] Polymerization condition: MAO/Zr = 2000, [Zr] = 2×10^{-5} mol/L; P_E = 1.013 bar, T = 30 °C.
[g] Polymerization condition: MAO/Ti = 1200–2500, [Ti] = 1×10^{-4} to 5×10^{-5} mol/L; P_E = 4 bar, T = 25 °C.

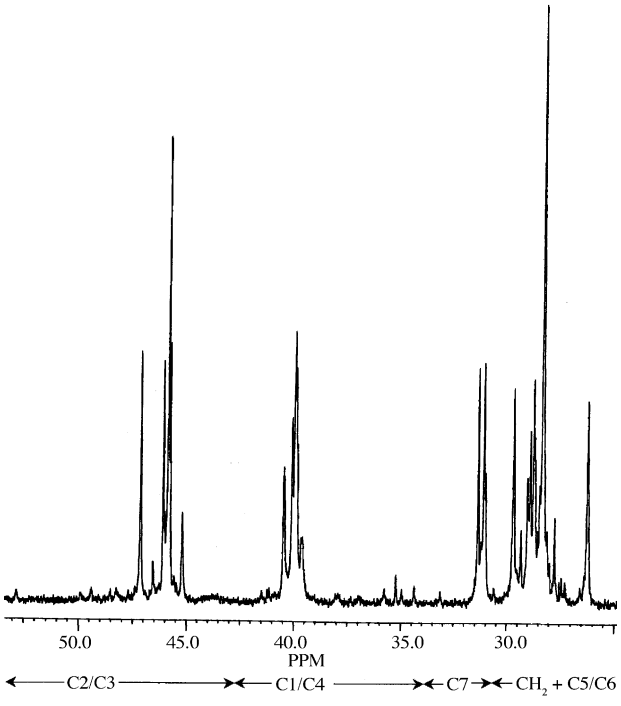

Fig. 5. ^{13}C NMR spectrum of an E–N copolymer, showing the four distinct zones corresponding, from left, to carbons C2/C3, C1/C4, C7, and ethene CH_2 and C5/C6. (Reprinted with permission from Macromolecules 33 (2000) 8931, Ref. [26].)

two strategies are available for the synthesis of mainly alternating copolymers which respectively consist in using: (i) catalysts with homotopic sites whose rate of homopolymerization of one monomer is faster than that of the other monomer; (ii) catalysts with heterotopic sites. The synthesis of alternating E–N copolymers was first disclosed by Cherdron without indication of the catalyst used [23]. Some relevant results of alternating E–N copolymerizations are reported in Table 1. Chart 3 shows examples of homotopic catalysts used for these syntheses. Catalyst *rac*-Me_2Si(2-Me-[*e*]-benzindenyl)$_2ZrCl_2$ (**I-6**) with C_2 symmetry has been already shown in Chart 2:

(i) *Catalysts with homotopic sites (C_s and C_2 symmetries).* Alternating E–N copolymers have been produced with "constrained geometry" catalyst (CGC) monocyclopentadienyltitanium amido $Me_2Si(Me_4Cp)(N^tBu)TiCl_2$ (**IV-1**) [32,33]. Bis(pyrrolide-imine)Ti (**VI**) complexes in conjunction with MAO produced mainly alternating E–N copolymers by living polymerization [34]: the high N affinity and the fast N insertion are thought to arise from the sterically open and highly electrophilic nature of the active site. New titanium complexes with two non-symmetric bidentate beta-enaminoketonato (N,O) ligands, [(Ph)NC(R-2)C(H)C(R-1)O]$_2TiCl_2$ (**VIII**) with a C_2-symmetric conformation [35], with modified methylaluminoxane (MMAO)

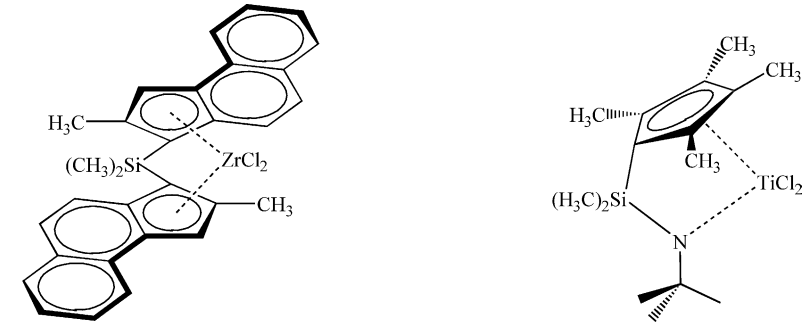

I-6

IV-1

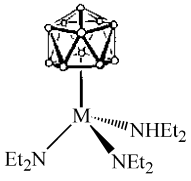

(M= Ti or Zr)

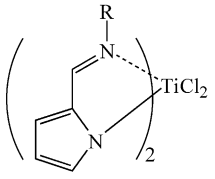

VI

R = (**VI-1**) (**VI-2**) (**VI-3**)

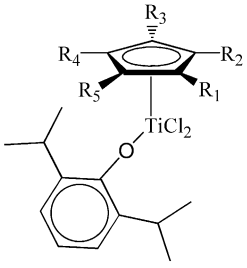

VII

$R_1, R_2, R_3, R_4, R_5 = CH_3$ (**VII-1**)
$R_1 - R_2$ = benzyl (**VII-2**)
$R_2 = {}^{t}Bu$ (**VII-3**)

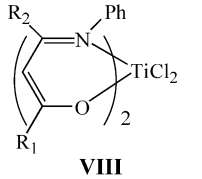

VIII

R_1 = Ph $R_2 = CF_3$ (**VIII-1**)
R_1 =  $R_2 = CF_3$ (**VIII-2**)
R_1 =  $R_2 = CF_3$ (**VIII-3**)
$R_1 = CF_3$, $R_2 = CH_3$ (**VIII-4**)

Chart 3. Examples of catalysts with homotopic sites utilized for the synthesis of alternating E–N copolymers.

as a cocatalyst, are capable of promoting the quasi-living copolymerization of ethene with norbornene at room temperature, yielding high molecular weight alternating copolymers with narrow molecular weight distributions. Other examples of catalysts yielding alternating E–N copolymers are dicarbollide catalysts ($\eta'^5C_2B_9H_{11}$) ($-C_2B_9H_{11}$)$M(NEt_2)_2$ ($NHEt_2$) (M = Ti or Zr) (**V**) [36] and non-bridged (aryloxo)-cyclopentadienyltitanium(IV) (**VII**) complexes [37].

The microstructure of these copolymers is atactic. Indeed, it is similar to that of copolymers obtained by $Me_2Si(Me_4Cp)(N^tBu)TiCl_2$ (**IV-1**), which was elucidated with the help of the correlation between ^{13}C NMR chemical shifts and average chain conformation computed by molecular mechanics and resulted to contain both *meso* and *racemic* NEN sequences [18].

Mainly alternating E–N copolymers have been obtained with the C_2 metallocene *rac*-Me_2Si(2-Me-[*e*]-benzindenyl)$_2ZrCl_2$ (**I-6**). This catalyst yields mainly isotactic alternating copolymers. ^{13}C NMR analysis and quantitative computation of polymer sequence distribution and tacticity demonstrated and quantified the major microstructural features and differences between copolymers obtained by catalysts **I-6** and **IV-1** [43]. The former alternating copolymer contains only *meso* NEN sequences, the tacticity of the alternating sequences being induced by the catalyst symmetry. Here, the formation of NN diads is disfavored but, surprisingly, a significant amount of NNN triads is observed.

Two trends common to all E–N copolymerizations by *ansa*-metallocenes are: (i) increase in N concentration in a

polymerization feed results in a decrease in catalytic activity, likely due to the facility of N coordination to the active sites, and in an increase of N content in the copolymer up to a plateau, which depends on the catalyst structure; (ii) molecular mass of the copolymer often increases with the increase of the norbornene content.

(ii) *Catalysts with heterotopic sites (C_1-symmetry).* The dual coordination sites of C_1-symmetric metallocenes was exploited by Arndt and Beulich [38], Fink and co-workers [39], and Harrington and Crowther [40] to control the sequence specificity in E–N copolymerization. Highly alternating stereoregular (isotactic) E–N copolymers have been synthesized with the C_1-symmetric, bridged metallocenes $R_2C(Flu)(3\text{-}R'Cp)ZrCl_2$ [R = Me or Ph, R′ = Me or ^{t}Bu] (**III-2–4**, **III-6**) [38,39] in the presence of an excess of norbornene, and with group 4 bridged monocyclopentadienyl catalysts such as μ-$Me_2Si(3\text{-}^t BuCp)$(adamantylamido)MMe_2 [M = Zr, or Hf] (**IX**) [40]. The copolymers prepared by Harrington are semi-crystalline with remarkably high melting points (250 °C) and show a very simple spectrum. The authors suggested that the crystallinity was originated from an alternating and stereospecific structure of the copolymer chain.

The copolymers prepared by Arndt and Beulich [38] and Fink and co-workers [39] with $R_2C(3\text{-}R'Cp)(Flu)\ ZrCl_2$ [R = Me or Ph, R′ = Me or ^{t}Bu] (**III-2–4**, **III-6**) are crystalline if the norbornene content is higher than 37 mol% and have melting points of 270–320 °C [38]. Elucidation of the microstructure of these copolymers showed that the enchainement of norbornene units is isotactic.

C_1-symmetric, bridged monocyclopentadienyl titanium amido complexes $Me_2Si(Cp')(N^tBu])TiCl_2$ (Cp′ = 2,4-Me_2Cp, 3-^{t}BuCp, indenyl) (**IV-2–4**) have also been shown to yield mainly alternating E–N copolymers by McKnight and Waymouth [32]. This systematic study showed that the catalyst having Cp′ equal to Me_4Cp is the most productive one. The nature of the ligand in this series had a little effect on the norbornene content and on T_g values. However, our inspection [18] of spectra of copolymers displayed in Fig. 9 of Ref. [32] reveals that the ligand substitution has a strong influence on the copolymer microstructure: the isotacticity in NEN sequences increases in the order **IV-1** < **IV-2** < **IV-3** < **IV-4**.

The behavior of pentalene metallocene in E–N copolymerization is reported by Prof. Kaminsky's review in this issue of Coordination Chemistry Review [41].

2.3.2. Signal assignments of alternating E–N copolymers

Fig. 6A shows the spectrum of an isotactic alternating copolymer prepared with $Me_2C[(3\text{-}^i Pr\text{-}Cp)(Flu)]ZrCl_2$ (**III-3**) presenting alternating *meso* NEN sequences. In Fig. 6B the spectrum of an isotactic alternating copolymer with similar norbornene content, synthesized with *rac*-$Me_2Si(2\text{-}Me\text{-}[e]\text{-benzindenyl})_2ZrCl_2$ (**I-6**), is reported for comparison. The spectra are relatively simple due to the prevailingly alternating erythrodiisotactic type of stereoregularity. Closer inspection of the spectrum in Fig. 6B shows smaller signals arising from NN diads and NNN triads.

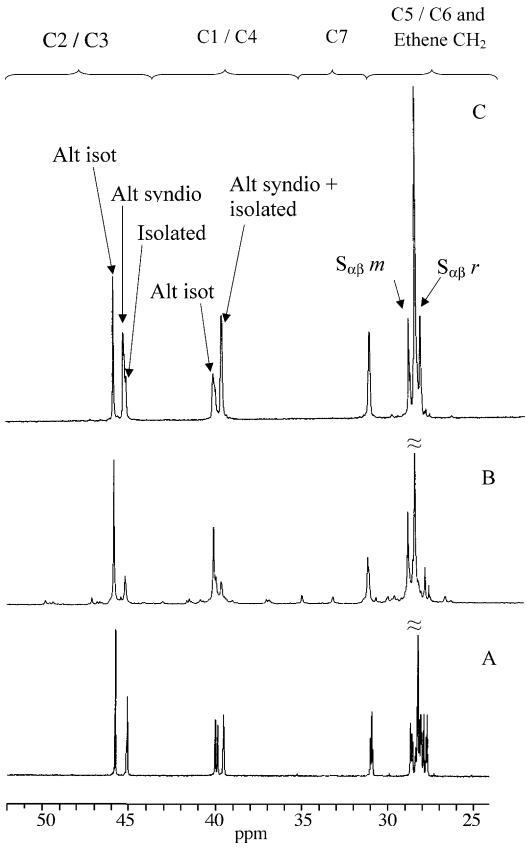

Fig. 6. ^{13}C NMR spectra of: (A) isotactic alternating copolymer prepared with $Me_2C[(3\text{-}^i Pr\text{-}Cp)(Flu)]ZrCl_2$ (**II-3**); (B) isotactic alternating copolymer with similar norbornene content synthesized with *rac*-$Me_2Si(2\text{-}Me\text{-}[e]\text{-benzindenyl})_2ZrCl_2$ (**I-6**); (C) copolymer prepared with $Me_2Si(Me_4Cp)(N^tBu)TiCl_2$ (**IV-1**) presenting alternating *meso* and *racemic* NEN sequences.

Fig. 6C shows the spectrum of a copolymer prepared with $Me_2Si(Me_4Cp)(N^tBu)TiCl_2$ (**IV-1**) presenting alternating *meso* and *racemic* NEN sequences.

An updated set of assignments of the ^{13}C NMR spectra of alternating erythrodiisotactic and erythrodisyndiotactic E–N copolymers is reported in Table 2. Besides the assignments published earlier by other authors and by us, Table 2 includes recent new assignments of $S_{\alpha\beta}$ methylenes of EENENEE, NENENEE, and NENENEN sequences and of the C2/C3 tertiary carbons in NENEE sequences [42].

At the onset of our studies, no mention of isotactic or syndiotactic types of regularity for alternating NENEN nor of *meso*/*racemic* norbornene diads (ENNE sequences) had been found in the literature. Substantial progress has come from the elucidation of the conformational structure of the chain of E–N copolymers by molecular mechanics calculations and from the correlation between conformation and ^{13}C NMR

Table 2
Assignments of ^{13}C NMR chemical shifts for carbons of norbornene and ethene units in alternating E–N copolymers

	Carbon[a]	Chemical shift (ppm)	Sequences	Ref.
Ethene				
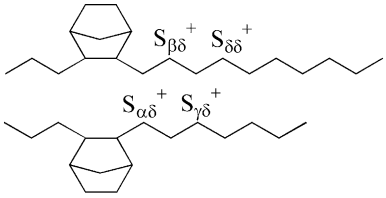	$S_{\delta+\delta+}$	27.74	EEE*E*EEE	[26]
	$S_{\delta\delta+}$	27.80	ENE*E*EE	[26]
	$S_{\beta\delta+}$	27.93	EN*E*EE	[18,20]
	$S_{\alpha\beta}$ *r*	28.04	EN*E*NE	[18]
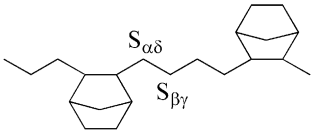	$S_{\gamma\delta+}$	28.05	ENE*E*E	[20,42]
	$S_{\alpha\delta+}$	28.13	EN*E*EE	[42]
	$S_{\alpha\delta+}$, $S_{\gamma\delta}$	28.18	EN*E*EN	[42]
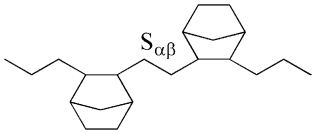	$S_{\beta\gamma}$	28.39	EN*E*EN	[18,20]
	$S_{\alpha\beta}$ *m*	28.56	EEN*E*NEE	[42]
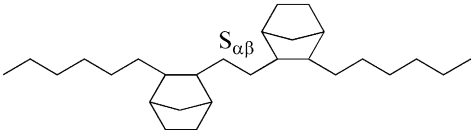	$S_{\alpha\beta}$ *m*	28.61	NEN*E*NEE	[42]
	$S_{\alpha\beta}$ *m*	28.66	NEN*E*NEE	[42]
	$S_{\alpha\beta}$ *m*	28.70	NEN*E*NEN	[42]
Norbornene				
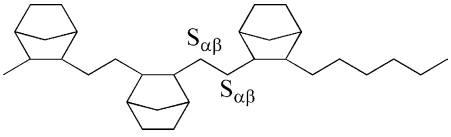	C5/C6	28.33	E*N*E	[18,20]
	C7	30.89	EE*N*EE	[26]
	C7 *m*	30.96	NE*N*EE	[39,46]
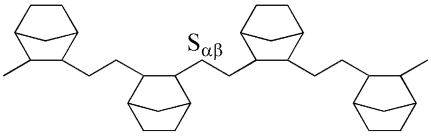	C7 *r*	30.98	NE*N*EN	[39,46]
	C7 *m*	31.04	NE*N*EN	[39,46]
	C1/C4 *r*	39.54	NE*N*EN	[18,20]
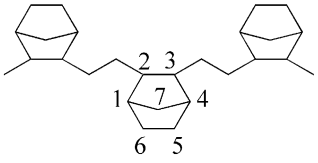	C4 *m*	39.54	1/2 NE*N*EE	[17,42]
	C1/C4	39.57	EE*N*EE	[26]
	C1 *m*	39.86	1/2 NE*N*EE	[42]
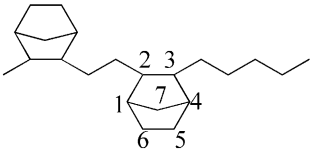	C1/C4 *m*	40.00	NE*N*EN	[18,20]
	C3 *m*	45.09	1/2 NE*N*EE	[42]
	C2/C3 *r*	45.21	NE*N*EN	[18,20]
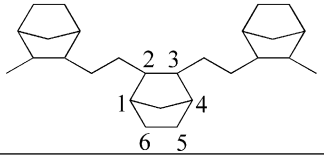	C2 *m*, C2/C3 *m*	45.78	1/2 NE*N*EE, NE*N*EN	[42]

[a] See Fig. 4 for the denomination of meso (*m*) and racemic (*r*) alternating NEN sequences.

chemical shifts [18]. Comparison of conformer populations computed for the stereoregular and stereoirregular polynorbornene and alternating $(N–E)_x$ chains and for copolymers including such defects as NN, E, EEE and NNN allowed us to predict stereochemical shifts. This led for the first time to distinguish between *meso* and *racemic* NEN sequences, namely to assign (a) the signals of the two norbornene methines C_2 and C_1 and of the ethene CH_2 in alternating *isotactic* and *syndiotactic* copolymers, (b) the isolated signals of the two methines of an N unit in a NEE$\cdots$ sequence and the $S_{\alpha\delta}$ signal, (c) the $S_{\beta\gamma}$ and $S_{\gamma\delta}$ signals shifted low field with respect to $S_{\beta\varepsilon}$ e and $S_{\delta\varepsilon}$, respectively.

While these studies were being completed, the results of the efforts of other groups in assigning ^{13}C NMR spectra of E–N copolymers have appeared in the literature [19]. Fink has distinguished and assigned the resonances of ethene carbons by comparing the ^{13}C NMR spectra of copolymers containing ^{13}C enriched ethene or ^{13}C enriched norbornene with those of copolymers prepared with monomers having natural ^{13}C abundance [20,19]. Arndt's assignments are based on the comparison of spectra of copolymers of naturally ^{13}C enriched monomers with various compositions obtained with different catalysts, in a manner analogous to our previous analysis [19].

Quite a general agreement on the assignments of ^{13}C NMR spectra of alternating copolymers was reached, apart from a disagreement on the assignments of three signals in the CH_2 region [24].

We have recently compared and discussed progress in such assignments [42]. A complete analysis of the spectra of copolymers with different norbornene content, where the relative peak areas of each spectrum are simultaneously best fitted, was carried out by using the procedure mentioned above [26,43]. It was possible to reconsider some controversial assignments of ethene CH_2 signals and to reach a new conclusion regarding signals $S_{\alpha\delta}$, $S_{\gamma\delta}$, and $S_{\gamma\beta}$ as summarized in Table 2. Our assignment regarding signals $S_{\alpha\delta}$ and $S_{\alpha\beta}$ is confirmed, but, as stated by Fink, it appears that signal $S_{\gamma\delta}$ does not overlap signal $S_{\gamma\delta+}$, but is shifted to lower field.

In Refs. [26,43], other regions of the spectra have been reconsidered and elucidated at higher resolution. In particular, the region of tertiary carbons C2/C3 between 45.09 and 45.78 ppm shows three distinct signals of the four expected at pentad resolution, while previous assignments only distinguished between isolated and alternating signals [38,44]. Several of these new assignments are in agreement with those reported by other authors [38,39,46].

The current level of assignments allows for the complete determination of the microstructure at pentad level if the information gathered from the whole spectrum is exploited. The information on a number of sequences is at heptad level. This fact may result in a more accurate estimate of the copolymerization parameters.

2.4. E–N copolymers containing norbornene blocks

2.4.1. Synthesis

Ansa-metallocenes with C_2 and C_s symmetries (Chart 2) generate random copolymers containing norbornene microblocks, although most *ansa*-zirconocenes produce mainly alternating E–N copolymers. Copolymers with norbornene content well above 50 mol% and T_g as high as 220 °C can be synthesized. Metallocene symmetry and ligand substituents dictate polymerization activity, tacticity, and sequential distribution. The type of bridge has an influence on polymerization activity and norbornene content. Examples, most of them taken from Kaminsky's report, are listed in Table 3 [47].

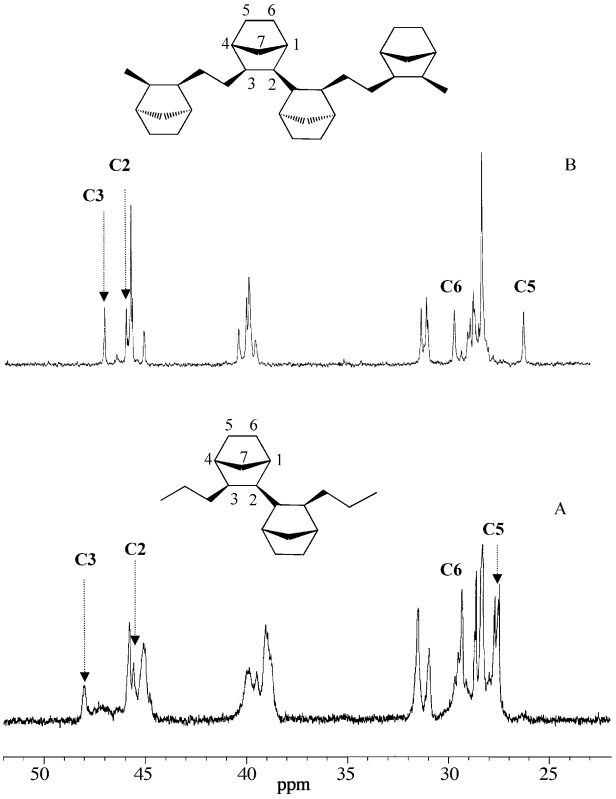

Fig. 7. ^{13}C NMR spectra of copolymers obtained by catalyst precursor **III-1** (A) and **I-2** (B).

The C_s symmetric $Me_2C(Cp)(Flu)ZrCl_2$ (**III-1**), $Me_2Si(Cp)(Flu)ZrCl_2$ (**III-5**), and $Ph_2C(Cp)(Flu)ZrCl_2$ (**III-6**), and the C_{2v} symmetric $H_2C(2,5\text{-}Me_2Cp)_2ZrCl_2$ [48] (**XII**) showed higher activity than the C_2 symmetric metallocenes. Among these catalysts most active is complex **XII**, while $Me_2Si(Cp)(Flu)ZrCl_2$ (**III-5**) shows the highest molecular mass [47].

The presence of a methyl substituent on α-carbons and the absence of substituents on the β-carbons in compound **XII** are crucial to the high activity of this system. The lack of steric hindrance on the reaction site facilitates the approach of the bulky norbornene to the reaction site and results in an increase of the norbornene content in the polymer. On the other side, compound $MeCH(Cp)_2ZrCl_2$ (**X**) [44] without methyl substituents was reported to have low activity and high norbornene incorporation ability. Among the C_2 symmetric metallocenes, *rac*-$Et(Indenyl)_2ZrCl_2$ (**I-2**) is the most active [3].

E–N copolymers prepared with C_2 symmetric **I-2** contain mainly *meso* ENNE diads and small amounts of *meso–meso* NNN triads. On the other hand, the C_s-symmetric $Me_2C(Flu)CpZrCl_2$ (**III-1**) based catalyst shows a high selectivity for producing E–N copolymers with *racemic* ENNE diads. In Fig. 7 the spectra of copolymers obtained by catalyst precursors **I-2** and **III-1** are compared. In the C2/C3 and C5/C6 regions the signals characteristic of *meso* EENNEE and *racemic* ENNE sequences are demonstrated.

Table 3
Random E–N copolymerization: activities and properties

Symmetry	Catalyst	Activity (kg pol/mol Zr h)	[*N*]/[*E*]	N mol% incorporated	T_g (°C)	M_w ($\times 10^{-4}$ g/mol)	Ref.
C_{2v}	**XI**	1200[a]	0.20	21	–	–	[3e,47]
	XII	68000[b]	6.12	–	171	13.0	[48]
		58000[b]	8.16	–	179	15.8	[48]
		26000[b]	12.24	–	196	16.4	[48]
		10000[b]	24.49	–	226	17.3	[48]
C_s	**III-1**	2210[c]	25.05	>56	175	12.7	[3b]
	III-5	11084[d]	19.0	47	129	43.1	[3e]
	III-6	2410[c]	25.05	>56	184	14.0	[3b]
	I-1	480[a]	0.20	28	75	–	[3e]
	I-2	9120[a]	0.20	26	72	22	[3,47]
		32[e]	24.0	55	173	–	[49,50,51]
C_s	**I-4**	2320[a]	0.20	28	40	–	[3e,47]
		1370[c]	3.21	35	82	18.8	[3b]
		290[c]	6.37	42	124	19.8	[3b]
		28[e]	24.0	58	168	–	[49,50,51]
	I-5	38[e]	24.0	54	194	–	[49,50,51]
	I-7	70[e]	24.0	60	148	–	[49,50,51]
	I-10	540[c]	3.21	34	86	14.7	[3b]
		90[c]	6.37	39	–	9.3	[3b]
	I-3	560[f]	12.5	36	–	11.3	[67]
	I-9	320[f]	12.5	0.5	–	8.6	[67]
C_1	**II-1**	2950[a]	0.20	33	–	–	[3e,47]
C_s	**IV-5**	176[g]	1.4	25	47	4.5	[52]
		480[g]	5.0	44	126	7.1	[52]
		675[g]	10.0	54	167	7.9	[52]

[a] Polymerization condition: MAO/Zr = 200, [Zr] = 5×10^{-6} mol/L; P_E = 2 bar, T = 30 °C.
[b] Polymerization condition: MAO/Zr = 4000, [Zr] = 5×10^{-5} mol/L, P_E = 1.72–6.89 bar, T = 60 °C.
[c] Polymerization condition: MAO/Zr = 1000, [Zr] = 5×10^{-7} mol/L; P_E = 2 bar, T = 30 °C.
[d] Polymerization condition: MAO/Zr = 8600, [Zr] = 5×10^{-6} mol/L, P_E = 2 bar, T = 30 °C.
[e] Polymerization condition: MAO/Zr = 2000, [Zr] = 1.6×10^{-5} mol/L, P_E = 1.013 bar, T = 30 °C.
[f] Polymerization condition: MAO/Zr = 1000, [Zr] = 8×10^{-5} mol/L; P_E = 1.013 bar, T = 30 °C.
[g] Polymerization conditions: MAO/Ti = 400, [Ti] = 6.6×10^{-4} mol/L, P_E = 1.013 bar, T = 20 °C.

Series of E–N copolymers were synthesized in the presence of zirconocenes with different symmetries and ligand patterns: *rac*-$Me_2Si(Indenyl)_2ZrCl_2$ (**I-4**), *rac*-$Me_2Si([e]\text{-benzindenyl})_2ZrCl_2$ (**I-5**) *rac*-$Me_2Si(2\text{-Me-}[e]\text{-indenyl})_2ZrCl_2$ (**I-7**), besides the already mentioned **I-2** and **III-1** [49–51]. The C_s symmetric **III-1**, as already known, resulted in the most productive catalyst. Among the C_2 symmetric catalysts, $Me_2Si(2\text{-Me-}[e]\text{-indenyl})_2ZrCl_2$ (**I-7**) was shown to be noticeably more active than the others of the series. The microstructure was dominated by metallocene symmetry and ligand type. Precursor **I-5** produced copolymers with the highest N content and the highest amount of *meso–meso* NNN sequences demonstrated in the spectrum of Fig. 8. The large number of signals is due to the increase of possible stereosequences as the norbornene block length increases. Present assignments of such signals to the specific configuration of C2/C3 carbons of norbornene triads are listed in Table 5.

As already mentioned, $Me_2Si([e]\text{-benzindenyl})_2ZrCl_2$ (**I-5**) gave the highest amount of *meso* ENNE sequence and no ENNNE in spite of high norbornene excess in the feed composition, while $Me_2Si(2\text{-Me-}[e]\text{-benzindenyl})_2ZrCl_2$ (**I-6**) gave a mainly alternating copolymer with trace amounts of ENNE sequences and a surprising higher amount of ENNNE sequences. Comparison of T_g of these copolymers having an N content between 48 and 60 mol% showed T_g values ranging between 125 and 194 °C. This work [51] led to the conclusion that there does not appear to be a linear correlation between the amount of N incorporated and the T_g measured when copolymers with high N content and different microstructures are considered.

The kinetics of E–N copolymerizations using a great number of metallocenes which include $Me_2C[(3\text{-}^i\text{Pr-Cp})Indenyl]ZrCl_2$/MAO (**II-2**) $MeCH(Cp)_2ZrCl_2$ (**X**), besides the already mentioned $Me_2C[(3\text{-R-Cp})(Flu)]ZrCl_2$ (with R = methyl or ^{t}Bu) (**III-2**, **III-4**), and CGC **IV-I**, have been investigated by Ruchatz and Fink [44] at 70 °C in a concentrated solution of norbornene and under an ethene pressure ranging from 4 to 60 bar. The highest norbornene content was achieved using metallocenes with sterically less demanding ligands such as $MeCH(Cp)_2ZrCl_2$ (**X**). Copolymers generated with metallocene $Me_2C[(3\text{-}^i\text{Pr-Cp})Indenyl]ZrCl_2$ (**II-2**) contain norbornene microblocks with a maximum length of two norbornene units. Depending on the catalyst struc-

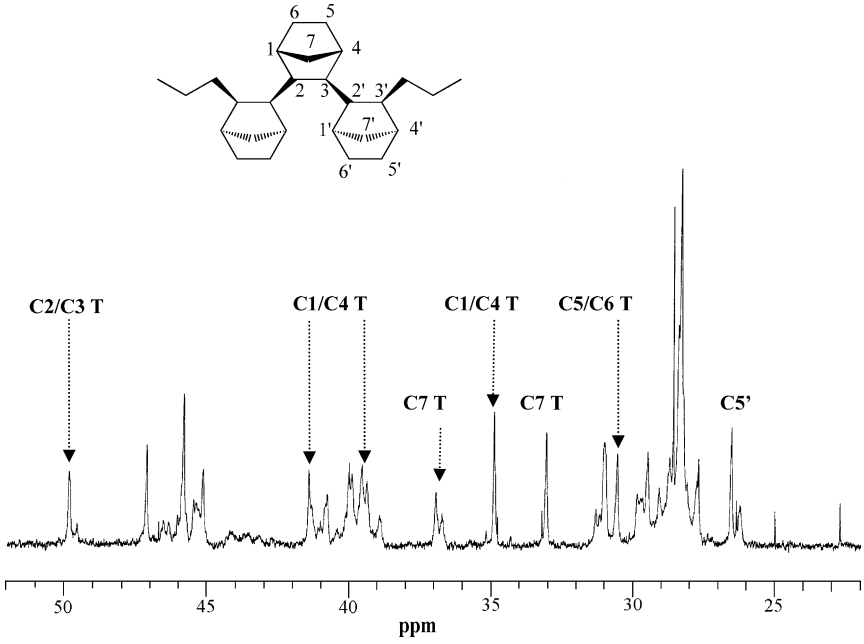

Fig. 8. ^{13}C NMR spectrum of a copolymer obtained by catalyst precursor Me_2Si(2-Me-[*e*]-indenyl)$_2ZrCl_2$ (**I-7**) showing *meso–meso* NNN sequences.

ture, the microstructure of the copolymers consists of mainly isolated norbornene units, alternating monomer sequences or short norbornene microblocks with a maximum length of two or three. Additionally, the tacticity of the norbornene microblocks could be controlled by the catalyst structure.

Wendt and Fink [45] carried out E–N copolymerizations at various ethene pressures by using the catalyst systems Me_2C[(3-^{i}Pr-Cp)Indenyl]$ZrCl_2$/MAO (**II-2**) and *rac*-Me_2C[Indenyl]$_2ZrCl_2$/MAO (**I-8**). Their analysis of the copolymer microstructures could conclude that, while copolymers obtained with metallocene Me_2C[(3-^{i}Pr-Cp)Indenyl]$ZrCl_2$ (**II-2**) contain only ENNE sequences, those generated with *rac*-Me_2C[Indenyl]$_2ZrCl_2$ (**I-8**) contain norbornene microblocks with a length of two or three. The amount of norbornene triblocks in the copolymer chain as well as the stereochemical connections of the norbornene triblocks were shown to depend on the monomer concentration and the polymerization temperature.

Recently, random E–N copolymers containing high norbornene content have been produced by Shiono and co-workers [52] by using Me_2Si(Flu)(N^{t}Bu)$TiMe_2$ (**IV-5**) activated with MAO free from Me_3Al. The ^{13}C NMR spectra of these copolymers showed new signals of triblock N sequences, which have been assigned to *rac*,*rac*-NNN triads.

2.4.2. Signal assignments of ENNE sequences in E–N copolymers

Table 4 collects our current signal assignments, achieved with the contributions by various authors, for the carbons involved in sequences with *meso* and *racemic* norbornene diblocks, along with sketches of the relative stereochemical sequences.

In particular, the spectra displayed above in Fig. 7 demonstrate the signals most characteristic of *meso* and *racemic* ENNE sequences. E–N copolymers prepared with *rac*-Et(Indenyl)$_2ZrCl_2$ (**I-2**) contain mainly *meso* ENNE diads revealed by the C2/C3 signals at 46.04 and 47.12 ppm characteristic of NENNEN which become more intense as the norbornene content increases. The two C2/C3 signals at 45.62 and 48.07 ppm, characteristic of *racemic* ENNE sequences, are present only in the spectrum of the copolymer obtained by Me_2C(Flu)$CpZrCl_2$ (**III-1**).

2D NMR spectra allowed Bergström et al. to recognize resonances of norbornene diblocks [23]. They first demonstrated C5/C6 and C2/C3 splittings in *meso* norbornene diads.

The comparison of ^{13}C NMR spectra of E–N copolymers of various composition prepared with different metallocenes initially allowed us to demonstrate the splitting of carbons belonging to racemic and meso ENNE sequences [50]. Then, examination of the complete ^{13}C NMR spectra of a great number of E–N copolymers, having various norbornene content (from 20 to 40%), by using a procedure based on least-squares fitting of all the peak areas of the spectra as described in Refs. [26,43], allowed us to further extend signal assignments: they include the signals of the C2/C3 carbons of EENNEE *meso* sequence and of carbons $S_{\alpha\beta}$ of NENNE sequences.

Arndt et al. [19] synthesized and assigned the ^{13}C NMR spectra of the stereoisomers of norbornene hydrodimers and hydrotrimers. These assignments have been very useful to assign signals in *meso* and *racemic* ENNE sequences. For example Arndt-Rosenau and Beulich compared a large number of spectra of copolymers prepared with C_2 and C_s symmetric metallocenes, with different norbornene con-

Table 4
Assignments of ^{13}C NMR chemical shifts for carbons of norbornene and ethene units affected by NN diads in E–N copolymers

	Carbon[a]	Chemical shift (ppm)	Sequences	Ref.
Ethene				
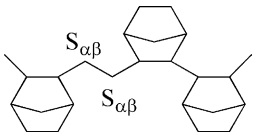	$S_{\alpha\beta}$ *m*	28.82	N*E*NN	[26]
	$S_{\alpha\beta}$ *m*	29.00	N*E*NN	[26]
Norbornene				
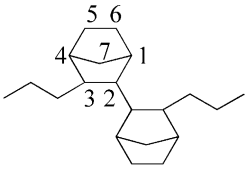	C5 *m*	26.24	ENNE	[26]
	C6 *m*	29.68	ENNE	[26]
	C7 *m*	31.17	ENNE	[26]
	C7 *m*	31.32	ENNE	[26]
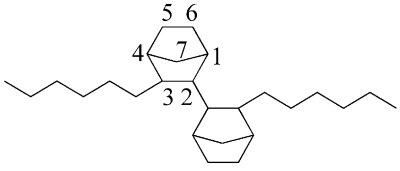	C1 *m*	39.88	ENNE	[26,44]
	C4 *m*	40.43	ENNE	[26,44]
	C2 *m*	45.96	EENNEE	[43,27]
	C2 *m*	46.05	NENNEN	[43,27]
	C3 *m*	46.50	EENNEE	[43,27]
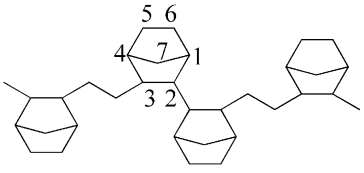	C3 *m*	47.12	NENNEN	[43,27]
	C5 *r*	27.58	ENNE	[26]
	C6 *r*	29.37	ENNE	[26]
	C7 *r*	31.57	ENNE[	[26]
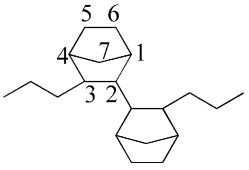	C1 *r*	38.93	ENNE	[26,44]
	C4 *r*	39.80	ENNE	[26,44]
	C2 *r*	45.62	ENNE	[43,27]
	C3 *r*	48.07	ENNE	[43,27]

[a] See Fig. 4 for the denomination of meso (*m*) and racemic (*r*) alternating NEN sequences.

tent to assign resonances of isotactic and syndiotactic norbornene diblocks [17]. On the basis of comparison of the copolymer chemical shifts with those of the stereoisomers of hydrodimers and hydrotrimers [19] they correctly assigned the signals of C1 and C4 carbons of *meso* and *racemic* ENNE sequences. However, on the basis of calculations on the most stable conformers by molecular mechanics and by considering such conformation-dependent effects as the well-known γ-gauche effect, we found that in order to simulate the copolymer chain a good model should have alkyl substituent in position 3,3′.

Conformer modelling demonstrated strong deformations of the norbornene rings in norbornene diads and triads and allowed us to ascribe the origin of stereo-chemical shifts due to NN and NNN sequences to the ring deformations arising from steric hindrance [50]. In particular, we understood the splitting of C5/C6 signals, the ring distortions being much stronger in *meso* diads than in the *racemic* ones, in agreement with Arndt-Rosenau and Beulich's assignments [17].

Ab initio calculations applied to proper model compounds confirmed that the splitting of signals of "internal" and "external" norbornene carbons in R–N–N–R compounds greatly depends on the nature of R as well as on the *meso–racemic* relationship of the N–N blocks. The 3,3′-di-*n*-propyl-dimers proved to be good models of ENNE sequences of E–N copolymers [27]. A comparison of experimental and ab initio computed chemical shifts of ENNE sequences is shown in Fig. 9.

2.4.3. Signal assignments of ENNNE sequences in E–N copolymers

Assignments of resonances of norbornene triblocks are even more complex and difficult than those of norbornene in alternating or diblock sequences.

Table 5 summarizes present assignments and working hypotheses found in the literature.

The first column reports the assignments currently used by us. The external carbons C5′ of *meso*, *meso* and *meso*, *rac* triads in ENNNE sequences were assigned by means of our best-fitting procedure for computing the stereosequence molar fractions [26]. In some cases we are able to distinguish *meso*, *meso* or *meso*, *rac* sequences without differentiating

Table 5
Assignments of ^{13}C NMR chemical shifts for carbons of norbornene and ethene units affected by NNN triads reported by different authors for E–N copolymers

This work and Ref. [26]		Ref. [24]		Ref. [52]	
Carbon	Chemical shifts (ppm)	Carbon	Chemical shifts (ppm)	Carbon	Chemical shifts (ppm)
		C6 *m,r*	26.31		
C5′ *m,m*	26.59[a]	C5/C6 *m,m*	26.50		
C5′ *r,m*	27.20–27.7	C5 *m,r*	26.8–27.4		
		C5′ *m,r*/C5′ *r,m*		C5/C6 *r,r*	28.09
C5/C6 T	29.37	C5′ *m,m*	29.4	C5/C6 *r,r*	29.12
C5/C6 T	29.49	C6′ *r,m*	29.62	C5/C6 *r,r*	29.56
		C6′ *m,r*	30.03		
C5/C6 T	30.50	C6′ *m,m*	30.5		
C5/C6 *m,m*	30.58				
		C7 *r,m*	32.87		
		C7 *m,m*	32.99		
C7 *m,m*	33.07			C7 *r,r*	33.11
C7 T	34.34	C7′ *r,m*	34.26		
C1/C4 *m,m*	34.92	C1/C4 *m,m*	34.87		
C1/C4 T	35.18	C4′ *r,m*	35.15		
C7 T	35.70	C7′ *m,r*	35.73	C7 *r,r*	35.55
C7 T *m,m*	36.74	C7′ *m,m*	36.67		
C7 T *m,m*	36.94				
C1/C4 T	36.94	C4′ *m,r*	36.89	C1/C4 *r,r*	36.87
				C1/C4 *r,r*	37.53
C1/C4 T	37.87	C1/C4 *m,r*	37.80	C1/C4 *r,r*	37.97
C1/C4 *m,m*	39.28–39.39				
C1/C4 T	40.80	C4′ *m,m*	40.77		
		C1′*r,m*	41.03		
C1/C4 T	41.32	C1′ *m,m*	41.18		
C1/C4 *m,m*	41.45				
C1/C4 T	41.56				
		C3′ *r,m*	42.64		
		C2′ *m,r*	43.55		
C2/C3 T	45.42	C3′ *m,m* (*NNNEE*)	45.49	C2/C3 *r,r*	45.62
	47.13	C3′ *m,r*/C2′ *r,m*	46.58/48.53		
		C3′ *m,m* (*NNNEN*)	48.22	C2/C3 *r,r*	48.74
C2/C3 T	49.34	C2 *m,r*	49.37		
C2/C3 *m,m*	49.80	C2′ *m,m*	49.83	C2/C3 *r,r*	49.51
C2/C3 T	50.00			C2/C3 *r,r*	50.92
C2/C3 *m,m*	52.70–52.84	C2/C3 *m,m*	52.78		
C2/C3 T	53.44	C3 *m,r*	53.41		

[a] Chemical shift referred to HMDS.

the single carbons. In other cases we simply assign signals to triads. Finally, in a few cases we rely on Fink's assignments.

The second column reports the detailed assignments achieved by Wendt and Fink [24]. The adopted numbering is the one shown in Fig. 3. The original chemical shifts values are shifted by −2.2 ppm. Such assignments were based on comparison between E–N copolymers prepared with *rac*-$Me_2Si(Indenyl)_2ZrCl_2$ (**I-4**), $Me_2C[(Cp)Indenyl]ZrCl_2$/MAO (**II-1**), and $Me_2C[(Cp\text{-}Flu]ZrCl_2$/MAO (**III-1**), with monomers with natural abundance of ^{13}C and with $^{13}C_{5/6}$-enriched norbornene. This methodology allowed Fink to assign resonances of NNN sequences with different stereochemical connections such as *meso*, *meso* and *rac*, *meso* [24]. In a first step DEPT experiments helped in distinguishing between the methylene (C7) or methine (C1/C4 and C2/C3) carbon atoms. Subsequently, by comparing spectra with different norbornene content and with the help of chemical shifts of norbornene hydrodimers and hydrotrimers synthesized by Arndt et al. [19] the authors obtained the assignments of *meso*, *meso* and *rac*, *meso* NNN sequences shown in the table.

Shiono synthesized random E–N copolymers containing high norbornene content by $Me_2Si(^tBuN)(Flu)TiMe_2$ (**IV-5**) [52]. The ^{13}C NMR spectra of these copolymers showed new signals which are listed in the last column of Table 5. On the basis of DEPT experiments, differences with previous spectra containing NNN sequences, differences in catalyst symmetries, and spectra of polynorbornene prepared with the same catalyst, the authors were able to assign these signals to *rac*, *rac*-NNN triads.

This result allows us to give an overview of the influence of Cp ligands and metallocene symmetry on the microstructure of E–N copolymers in Scheme 2. This completes the scheme given in Fig. 14 in Ref. [24].

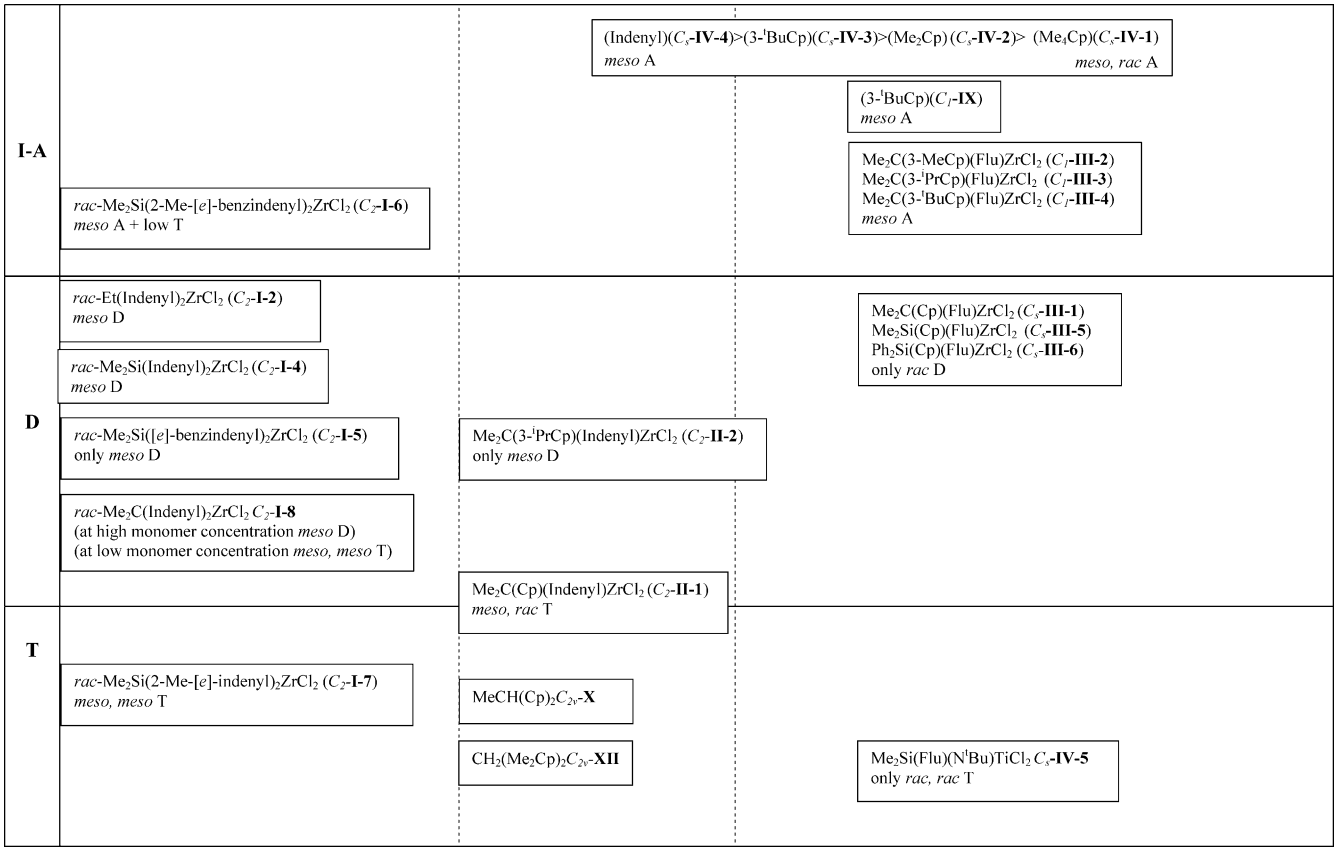

Scheme 2. Influence of metallocene ligands on the microstructures of E–N sequences: I = N isolated units; A = NEN alternating, D = ENNE, T = ENNNE sequences.

2.5. Copolymerization statistics

Copolymerization propagation kinetics can be described by Markov statistics, the first and second-order Markov models being most frequently used. When the insertion of a comonomer is influenced only by the last inserted unit [53] the first-order Markov model is sufficient to describe the copolymerization and the following two reactivity ratios are defined:

$$r_1 = k_{11}/k_{12} = k_{EE}/k_{EN} \quad \text{and} \quad r_2 = k_{22}/k_{21} = k_{NN}/k_{NE},$$

where k_{mn} represents the rate constant for the insertion of monomer n into an m-metal ended chain.

When the insertion of a comonomer is influenced by the penultimate unit, then the second-order Markov statistical model is needed to describe the copolymerization and four reactivity ratios are defined:

$$r_{11} = k_{111}/k_{112} = k_{EEE}/k_{EEN} \quad \text{and}$$
$$r_{22} = k_{222}/k_{221} = k_{NNN}/k_{NNE}$$

$$r_{21} = k_{211}/k_{212} = k_{NEE}/k_{NEN} \quad \text{and}$$
$$r_{12} = k_{122}/k_{121} = k_{ENN}/k_{ENE},$$

where k_{lmn} represents the rate constant for the insertion of monomer n into an lm-metal ended chain.

The most used methods for determining the copolymerization parameters utilize the Finemann and Ross [53] and Kelen–Tüdos [54] equations, which correlate the feed ratio to the copolymer composition. Several copolymerizations of ethene and norbornene need to be carried out with a given catalyst over a broad range of the comonomer ratio. However, since for the Fineman–Ross method a terminal copolymerization model has to be valid, only the r_1 and r_2 reactivity ratios can be obtained. The same holds for the Kelen–Tüdos method which consists in the linearization of the Finemann and Ross equation. Copolymerization parameters can be derived also from the analysis of a single ^{13}C NMR spectrum if it allows one to determine the sequence distribution. The knowledge of the triad distribution provides the r_1 and r_2 parameters, while it allows one to measure, but not to test, the four copolymerization parameters of a penultimate model. Indeed, at least the complete tetrad distribution is required to test [55] both the first-order (herein after indicated as M1) and the second-order Markov (M2) statistics. Computer analysis allows a best fit between the experimental sequence distribution and the one predicted by the statistical models. Of course, the more detailed is the microstructural information of the copolymer chain, the more

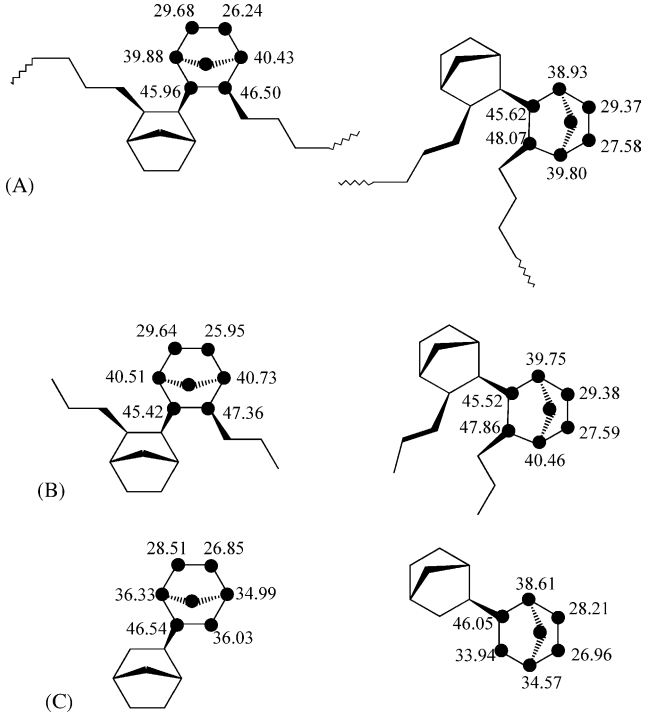

Fig. 9. Comparison of the chemical shifts (ppm) (A) of EENNEE sequences of E–N copolymers taken from Table 4, (B) computed ab initio for 3,3′-di-*n*-propyl N dimers; the values of Table 5 in Ref. [27] for C5/C6, C2/C3, and C1/C4 shifted by −4.87, −6.09, and −5.96 ppm, respectively, (C) of hydrodimers values by Arndt et al. [19] shifted by −2.2 ppm to account for the difference in internal reference.

detailed information on the copolymerization kinetics and the deeper insights in the copolymerization mechanisms can be reached.

2.5.1. E–N reactivity ratios from Finemann and Ross

Most authors have calculated the E–N reactivity ratios according to the Fineman–Ross method. Examples of the reactivity ratios so obtained are collected in Table 6. McKnight and Waymouth found that four CGC catalysts give r_1 values between 2.0 and 5.1 [32]. The values found are consistent with values for ethene/octene copolymerizations ($r_1 = 2.6$–4) with the same catalysts [56] and indicate a preference for the insertion of ethene over norbornene into a Mt–E* active center. In no case it was possible to accurately determine r_2 from the plots. However, the data were consistent with a value of r_2 very close to zero. The product of the reactivity ratios for all the CGC E–N systems approaches zero, indicating a tendency toward alternation.

Kaminsky et al. [57] and Ruchatz and Fink [58] have investigated the reactivity ratios of various metallocene catalysts known to incorporate more than 50 mol% norbornene at high norbornene feed concentrations (>80 mol%). Waymouth found similar trends in reactivity ratios; however, the r_1 values found under different conditions are lower. Differences

Table 6
Reported E–N reactivity ratios from Finemann and Ross equation

Symmetry	Catalyst	r_1	r_2	Ref.
C_s	**IV-1**	2.4	∼0	[32]
C_1	**IV-2**	1.9	∼0	[32]
	IV-3	5.1	∼0	[32]
	IV-4	2.2	∼0	[32]
C_{2v}	**XI**	20	–	[3]
		4.0	0.03	[32]
C_1	**II-1**	0.88	0.05	[57]
C_2	**I-1**	2.2	–	[3]
	I-2	6.6	∼0	[3]
		1.9	0.03	[32]
	I-4	2.66	0.36	[3,47]
	I-10	3.44	–	[3]
C_s	**III-6**	2.61	–	[3]
	III-1	2.93	–	[3]
		1.8	∼0	[32]
		1.3	0.03	[57]
C_1	**III-4**	3.3	0.001	[3]

in the calculated r_1 values with respect to those previously reported (Table 6) were attributed to the different reaction temperatures.

Bridged zirconocenes **I-2** and **III-1** have r_1 values near 2.0 similar to the CGC catalysts **IV-1**, **IV-2**, and **IV-4**. Catalyst Cp_2ZrCl_2 (**XI**) has an r_1 value of 4.0, reflecting the steric influence of the unbridged cyclopentadienyl rings. These r_1 values for all the three catalysts indicate a preference for insertion of ethene over norbornene into an active Mt–E* center. For **I-2** and **XI** Waymouth et al. calculated an r_2 value of 0.03, while for **III-1** the r_2 value is very close to zero. This clearly illustrates that these catalysts also disfavor a second norbornene insertion because of the steric influence of the last inserted norbornene unit. Like the CGC catalysts, these zirconocenes should have a tendency to produce alternating microstructures at high N/E feed ratios. Actually, the ^{13}C NMR spectra in Fig. 7 clearly reveal that catalysts **I-2** and **III-1** are able to produce copolymers with ENNE sequences.

Kaminsky et al. [57] found that bridged *rac*-$Me_2Si(Indenyl)_2ZrCl_2$ (**I-4**) yields copolymers with an r_1 value of 2.66 and an r_2 value of 0.36, which are a clear indication of the random nature of the copolymers obtained.

All the C_1 symmetric catalysts **III-2**, **III-3**, and **III-4** have r_1 values between 2.7 and 3.3, the only r_2 value in the table is 0.001 for **III-2**. Owing to the highly alternating nature of these copolymers the r_2 values could not be calculated by the Finemann and Ross equations.

A computer optimization routine was employed by us [59] to derive the reactivity ratios for both first- and second-order Markov models by fitting the theoretical equations relating copolymer composition and feed composition to the corresponding experimental data. The reactivity values agree with the reports that E–N copolymers obtained with **IV-1**/MAO

are mainly alternating ($r_1 \times r_2 \ll 1$), the norbornene diad fraction is very low, and there are no norbornene triads or longer blocks ($r_2 \approx 0$).

2.5.2. E–N reactivity ratios from tetrad analysis

The accuracy of the complete description of the copolymer microstructure at tetrad level with a standard deviation of 1–2% [60] allows one to identify the statistical model most suitable to describe the copolymerizations as well as to derive the reactivity ratios between the two comonomers. In contrast to the Finemann and Ross method [35] the available tetrad information allows us to test both the M1 and M2 statistics [55].

Both models were applied to fit the experimental tetrad distributions of a number of copolymers obtained from catalysts **I-2**, **I-4**, **I-6**, and **IV-1**. In order to examine the dependence of the copolymerization parameters on the feed ratio, the data of each sample were fitted separately.

The results on the reactivity ratios regarding two samples per catalyst are summarized in Table 7. The ranges of the reactivity ratios obtained at the lowest N/E feed ratio are: $r_1 = 2.34$–4.99, $r_2 = 0.0$–0.062. These values are within the same range of those reported in the literature, obtained with the Finemann and Ross method. The r_2 values are in general smaller than those obtained for propene copolymerization. The highest $r_1 \cdot r_2$ values found for the copolymers prepared with catalyst **I-4** confirm its tendency to give more random copolymers. The values of r_1, r_2, and $r_1 \cdot r_2$ for the E–N copolymers obtained with catalysts **IV-1** and **I-6** are comparable with those of alternating ethene-propene copolymers with metallocene catalysts [61]. It is worth observing the difference in copolymerization parameters obtained under different monomer feed ratios. Such differences suggest that the type of penultimate unit is indeed important in E–N copolymerizations. Such indications are confirmed by inspection of Table 7, where the results of the second-order Markov model are reported. As r_1, also all r_{11} values are similar to those found for ethene and propene copolymerization with metallocene catalysts with low reactivity ratios [61]. Differences in r_{12} and in r_{22} are illuminating, since they clearly show the preference of the insertion of E or N into E–N–Mt and N–N–Mt, respectively. Parameter r_{12} increases in the order **IV-1** < **I-6** ≪ **I-2** < **I-4**, opposite to the tendency to alternate the two comonomers [60].

The r_{22} values are in general lower than those obtained for propene or other α-olefins, in agreement with the low homopolymerization activity of norbornene. The r_{22} value for catalyst **I-6** is much greater than r_{12}; this shows the tendency of this catalyst to insert a third norbornene after the second one. In addition, the four copolymerization parameters calculated for the copolymers prepared with **I-2** and **IV-1** are quite independent of monomer concentrations, while those for copolymers obtained with **I-4** and **I-6** at two different monomer concentrations are quite different.

The experimental tetrad distributions and those calculated according to first- and second-order Markovian models are compared in Fig. 10. These comparisons and the rms deviations in Table 7 help us to discriminate between first- and second-order Markov models. Worthy of note is the very good agreement between all the tetrads calculated with the second-order model and the experimental tetrads – *isolated* (ENEE), *alternating* (NENE), and *block* (NNEN, ENNE, NNNE) – in copolymers from **I-2**, **I-4**, and **IV-1**. In contrast, the rms for the alternating copolymers produced from **I-6** are not satisfactory either with first- or with second-order models. This appears to confirm our previous hypothesis that various mechanisms are at work with this catalyst [43]. Finally, it is worth noting that these results indicate that r_{11}, r_{12}, r_{21}, and r_{22} can be dependent on the feed composition, suggesting that at high N/E ratio the reactivity of the propagating species can

Table 7
Reactivity ratios of E–N copolymerizations calculated using first- and second-order Markov models from tetrad and pentad distributions[a]

Symmetry	Catalyst	[N]/[E]	N mol% incorporated	Reactivity ratios								
				r_1	r_2	$r_1 \cdot r_2$	Fit[b]	r_{11}	r_{12}	r_{21}	r_{22}	Fit[b]
C_2	**I-2**[c]	2.33	36.23	2.602	0.0275	0.072	0.0111	3.048	0.0247	2.386	0.0081	0.0070
		3.98	40.38	2.338	0.0309	0.072	0.0101	3.241	0.0298	2.191	0.0176	0.0037
	I-4[c]	2.33	33.85	2.717	0.0525	0.143	0.0095	3.046	0.0489	2.519	0.1393	0.0060
		3.98	40.52	2.871	0.0618	0.177	0.0137	4.174	0.0622	2.543	0.0339	0.0013
	I-6[c]	2.33	29.72	3.338	0.0071	0.024	0.0118	3.486	0.0061	3.207	0.6179	0.0110
		9.74	41.18	4.477	0.0043	0.019	0.0141	6.805	0.0035	4.211	0.0809	0.0096
C_s	**IV-1**[c]	2.33	27.20	3.906	0	0	0.0265	3.232	0	5.184	0	0.0029
		3.98	31.79	4.988	0	0	0.0362	3.376	0	6.521	0	0.0024
C_1	**III-2**[d]	2.13	28.71	3.17	0	0	0.0154	3.46	0	2.76	0	0.0100
		3.62	35.23	2.94	0	0	0.0286	3.89	0	2.52	0	0.0166
	III-3[d]	2.33	23.93	5.34	0	0	0.0309	5.93	0	3.61	0	0.0215
		4.00	30.95	5.00	0	0	0.0428	6.93	0	3.33	0	0.0127

[a] [Zr] = 0.010 mmol/L; [Al]/[Zr] = 3000; P_E = 1.013 bar; T = 30 °C; solvent = toluene.
[b] Defined as root mean square deviation between computed and experimental tetrad or pentad fractions [Fit = $(\Delta/10)^{1/2}$] [60].
[c] From tetrad level analysis of ^{13}C NMR spectra [60].
[d] From pentad level analysis of ^{13}C NMR spectra [42].

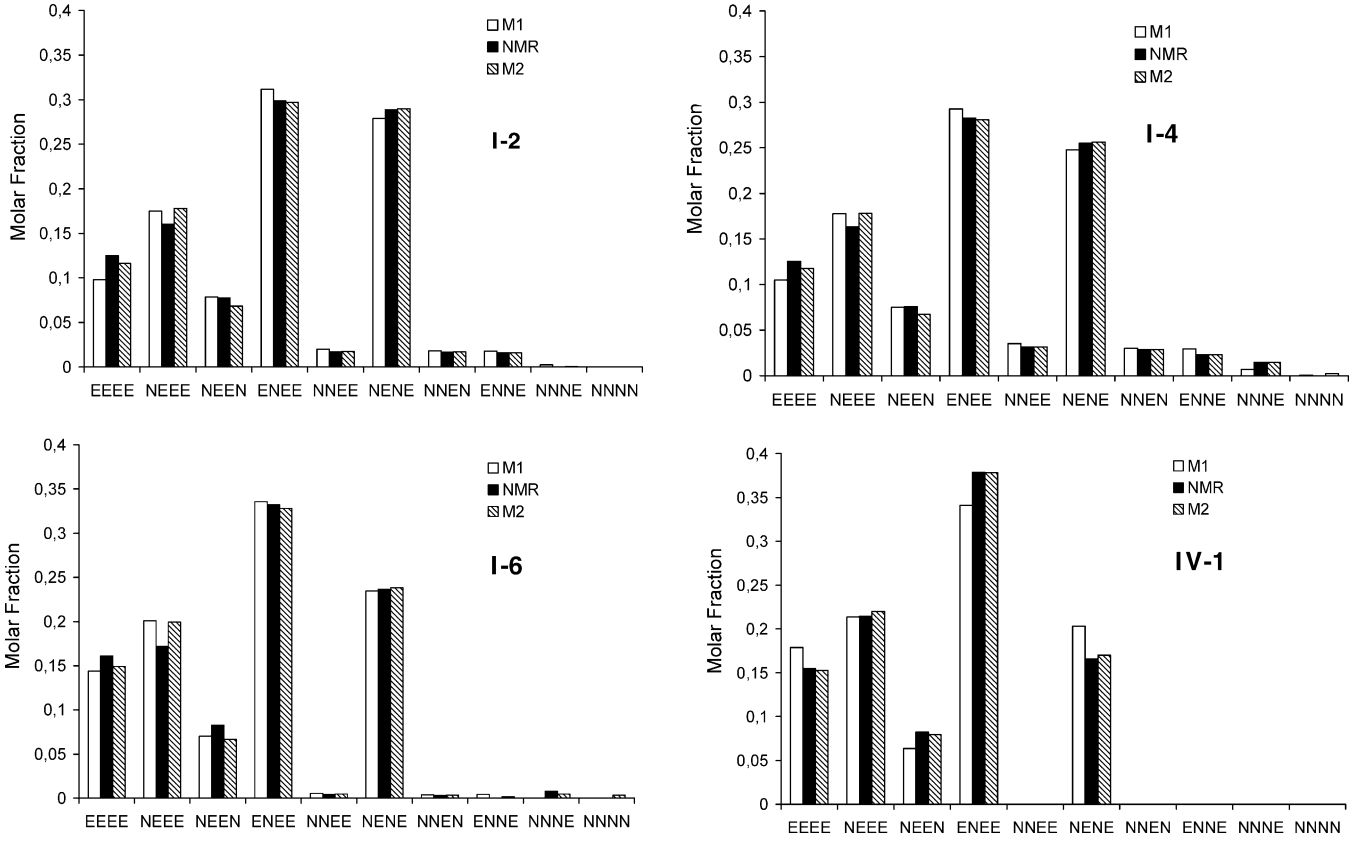

Fig. 10. Tetrad distributions for E–N copolymers, observed by NMR and calculated for samples prepared with *rac*-Et(Indenyl)$_2$ZrCl$_2$ (**I-2**), *rac*-Me$_2$Si(Indenyl)$_2$ZrCl$_2$ (**I-4**), *rac*-Me$_2$Si(2-Me-[e]-benzindenyl)$_2$ZrCl$_2$ (**I-6**) and Me$_2$Si(Me$_4$Cp)(N^{t}Bu)TiCl$_2$ (**IV-1**) at feed ratio 2.33. Black: experimental data; white: according to first-order Markov model; dashed: according to second-order Markov model.

be influenced by effects more distant than the penultimate monomer unit.

These results allowed us to clarify the statistics of these copolymerizations and to discriminate between ultimate and penultimate effects. It is possible to state that the next-to-last E or N monomer unit exerts an influence on the reactivity of the propagating Mt–E* or Mt–N* species. Such an influence seems to be contingent upon the catalyst structure. The second-order Markov model must be used to describe E–N copolymerizations promoted by metallocenes **I-2**, **I-4**, and **IV-1**. A third-order or a more complex model may be required to fit the experimental data obtained with catalyst **I-6**, where more sterically hindered indene substitutions are dominant. At higher norbornene concentrations, copolymers with all catalysts may need more complex models. These results are sufficient to conceive that E–N copolymerization is dominated by the bulkiness of the norbornene monomer and of the copolymer chain.

2.5.3. E–N reactivity ratios from pentad analysis

We have recently used the pentad description of the microstructure of the alternating copolymers prepared with catalysts **III-2** and **III-3** to test different copolymerization mechanisms. Catalysts **III-2** and **III-3** are two of the typical C_1 symmetric catalysts, such as Me$_2$C[(3-R-Cp)(Flu)]ZrCl$_2$ (R = Me, ^{i}Pr, ^{t}Bu), which produce *isotactic alternating* E−N copolymers [38,39]. The analysis of these has been used to elucidate polymerization mechanistic details such as the importance of *chain migration mechanism* versus *chain retention mechanism* [38,24]. Arndt and Beulich [38] used a statistical model which differentiates two heterotopic sites of the catalyst Me$_2$C[(3-^{t}Bu-Cp)(Flu)]ZrCl$_2$ (**III-4**): one site, always in the Zr–E* state, follows M1 statistics; the second one can be in both Zr–E* and Zr–N* states and follows M2 statistics. This mechanism allows for the formation of only odd ethene blocks. He concluded that E–N copolymerization follows a chain migration mechanism. On the other hand, Fink and co-workers [39] have recently analyzed at triad level the E–N copolymer spectra obtained with Me$_2$C[(3-^{i}Pr-Cp)(Flu)]ZrCl$_2$ (**III-3**) by using their assignments [24]. From a comparison of the root-mean-square residuals which correlate experimental and theoretical triad molar fractions calculated according to M1 and M2 Markov statistics, they concluded that E–N copolymerization with this catalyst follows M1 statistics and occurs according to a chain *retention* mechanism.

We have used our pentad level information on these copolymers to test M1 and M2 statistics as well as the two-

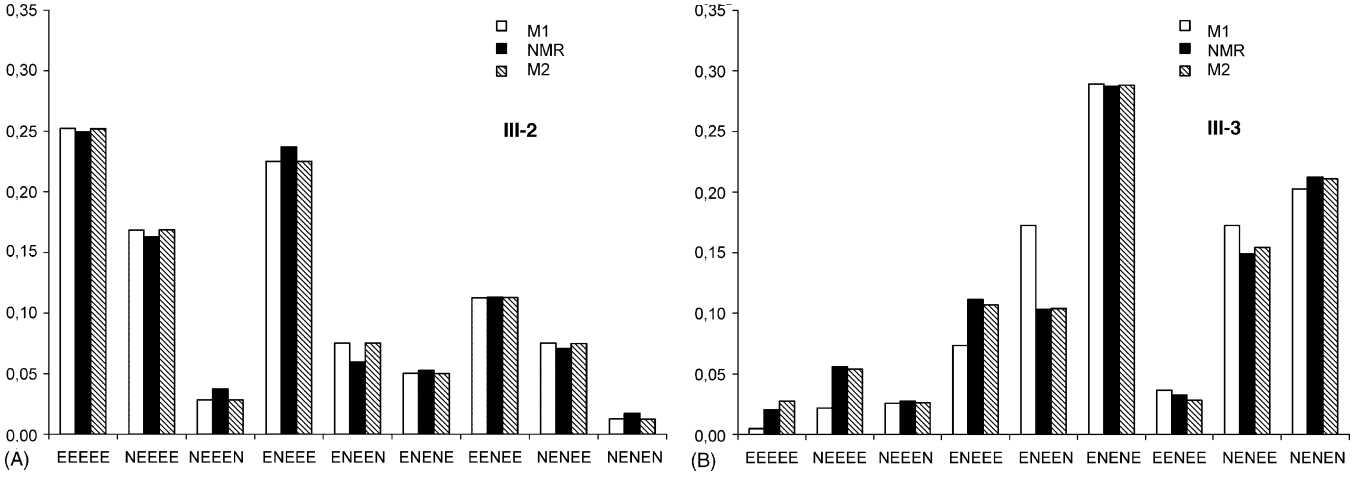

Fig. 11. Pentad distributions for E–N copolymers, observed by NMR and calculated for samples prepared (A) with *i*-Pr(3-MeCp)(Flu)$ZrCl_2$ (**III-2**) and (B) *i*-Pr(3-Pr^{i}Cp)(Flu)$ZrCl_2$ (**III-3**), at feed ratio 2.33. Black: experimental data; white: according to first-order Markov model; dashed: according to second-order Markov model.

site alternating mechanism (TSAM) proposed by Arndt. The fitting estimated standard errors showed that the two-site alternating mechanism is not valid for E–N copolymerization with both catalysts [42].

The results, partially shown in Table 7, clearly indicate that the second-order Markov statistics is more appropriate to describe the series of copolymerizations with catalyst **III-3**. On the contrary, it turns out that the M1 statistics is sufficient to describe the copolymerization with the Me-substituted metallocene **III-2**, at least for copolymers prepared at not too high feed ratios. Indeed, differences in the fitting between M1 and M2 are so small for copolymers prepared by **III-2** that r_{11} and r_{21} are similar to r_1. This indicates that when Cp is substituted with the small methyl substituent the penultimate inserted unit does not have any influence on the selection of the next unit.

These features are more evident in Fig. 11, where the NMR-measured pentad distributions obtained by our methodology (with assignments of Table 2) are compared with those calculated according to first- and second-order Markovian models. One representative copolymer sample produced by **III-3** and one produced by **III-2** were selected for such a comparison.

It is clear that: (i) sequences with even ethene units ENEEN are present in the two copolymers, thus ruling out the two-sites alternating mechanism for E–N copolymerization with these catalysts; (ii) the M1 statistics accurately describes the copolymer sample derived from catalyst **III-2**; (iii) the M2 statistics is necessary to describe the copolymer microstructure of the copolymer sample produced by **III-3**.

2.5.4. E–N reactivity ratios from Choi's method

Choi et al. developed a novel kinetic model to quantify the behavior of the copolymerization process [62] which confirmed the validity of the M2 statistics (penultimate model) that we obtained from the microstructural analysis of E–N copolymers at tetrad level.

They investigated the kinetics of E–N copolymerization to cyclic olefin copolymer using the *rac*-Et(Indenyl)$_2$$ZrCl_2$/methylaluminoxane catalyst in toluene at 70 °C for N/E mole ratios in the range of 3–55. The reactivity ratios ($r_1 = 1.47$, $r_2 = 0.024$) obtained using the terminal model give a reasonably good prediction of copolymer composition; however, the terminal model fails to accurately predict the polymerization rates of ethene and norbornene. To overcome the limitations of the terminal model the authors developed a penultimate model. The relevant kinetic parameters were estimated using experimental data and an optimal parameter estimation technique. The penultimate model simulation results show that the model fits the experimental data very well. The penultimate model calculations also indicate that the E–N polymerization process shows different kinetic behaviors below and above the bulk phase norbornene concentration of about 50 mol%. Most importantly the authors could show that the penultimate model, unlike the terminal model, correctly predicts the existence of a maximum norbornene polymerization rate.

2.6. Mechanisms

2.6.1. Alternating copolymers from catalysts with heterotopic sites (C_1-symmetry)

Polymerization statistics from pentad description of the microstructure of the *isotactic alternating* E–N copolymers prepared with C_1 symmetric catalysts Me_2C[(3-R-Cp)(Flu)]$ZrCl_2$ (R = Me, ^{i}Pr) **III-2** and **III-3**, used to test different copolymerization mechanisms, rules out that the synthesis of these copolymers can derive from a TSAM mechanism [38], according to which, as in Cossee's mechanism [63], the polymer chain migrates to the site where the monomer was initially coordinated [64].

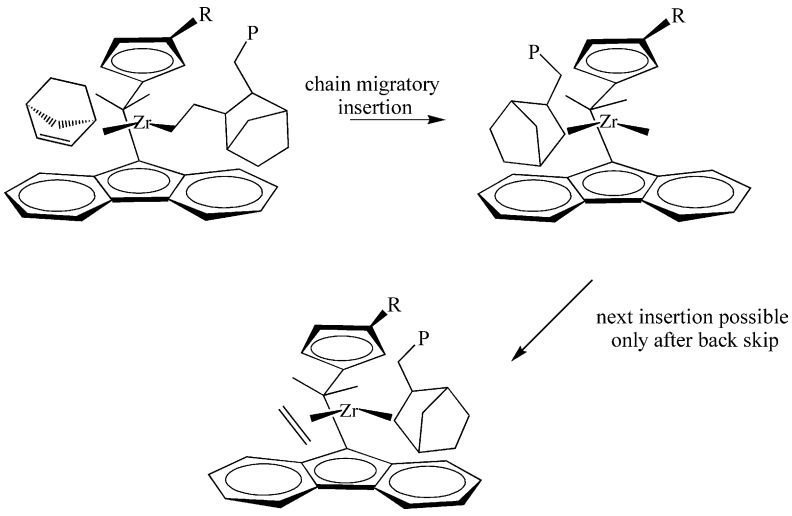

Fig. 12. Copolymerization mechanism for E–N copolymerization with C_1 symmetric catalysts. (Reprinted with permission from Macromolecules 37 (2004) 9681–9693, Ref. [42].)

The analysis of the microstructures of isotactic alternating E–N copolymers reveals that the synthesis of the copolymers prepared with both **III-2** and **III-3** comes from a retention mechanism, confirming Fink's observation. Thus, these C_1-symmetric catalysts behave as single-site catalysts and both ethene and norbornene are inserted at the same site, bringing to isotactic NENEN sequences. The microstructure of E–N copolymers produced by $Me_2C[(Cp)(Flu)]ZrCl_2$ (**III-1**), which may have N content well above 50%, and contain ENNE sequences only *racemic*, is convincing evidence that also for E–N copolymerizations the olefin insertion involves the migration of the polymer chain to the site occupied by the coordinated monomer (a Cossee-type mechanism). This implies that the E–N copolymer chain produced by catalysts **III-2** and **III-3**, independently of the last inserted unit, has to skip back to its original site before the next monomer can be inserted at the same site. It seems reasonable that norbornene and ethene are inserted on the more open site following Cossee's migratory mechanism and the copolymer chain after every insertion occasionally skips back to a less stable state, explaining the slow kinetics of E–N copolymerization (Fig. 12). The synthesis of alternating E–N copolymers, possible only at very high N/E feed ratios, derives from the impossibility of having two consecutive norbornene insertions. The isotacticity is a consequence of norbornene being inserted always at the same site with the same face.

2.6.2. Alternating copolymers from catalysts with homotopic sites (C_s and C_2-symmetry)

The mechanistic information from the analysis of copolymers with heterotopic sites probably holds also for catalysts with homotopic sites. The C_2-symmetric bridged metallocene *rac*-Me_2Si(2-Me-[*e*]-benzindenyl)$_2ZrCl_2$ (**I-6**) with two homotopic sites yields mainly isotactic alternating copolymers, in contrast to other C_2-symmetric bridged metallocenes such as *rac*-$Me_2Si(Indenyl)_2ZrCl_2$ (**I-4**), which give rise to more random copolymers under the same conditions. The catalyst symmetry induces the tacticity of the alternating sequences. The bulkiness of the catalyst ligands, of the growing polymer chain, and of norbornene seems to cause strong non-bonded interactions which explain the limited formation of norbornene diads.

It is more difficult to guess the nature of the interactions which after two successive norbornene insertions with the bulky catalyst **I-6** favor the insertion of a third norbornene unit. The presence of NNN triads in a mainly alternating copolymer seems to indicate that various mechanisms are at work for this C_2 symmetric catalyst. A third-order or a more complex model may be required to fit the experimental data obtained with catalyst **I-6** where more sterically hindered indene substitutions are dominant. Such a surprising structure confirms the great potential of metallocene catalysts in tailoring polymer structure.

On comparing the structures of the two catalysts **I-6** and **IV-1**, it seems reasonable that the permethylation of the Cp ligand increases the steric crowding at the upper half of **IV-1**, which could push the growing polymer chain towards the lower half, that is, towards the same side which should favor the norbornene approach. From this perspective, addition of a second norbornene unit should be much more hindered with respect to the insertion of an ethene unit, after a first insertion of norbornene. This could thus explain why the CGC produces a much more alternating copolymer. The presence of both *meso* and *racemic* NEN sequences and *meso* and *racemic* NN diads could be explained by similar probabilities for norbornene to coordinate and insert at the left or the right coordination sites.

2.6.3. Random copolymers

The formation of *racemic* NN diads from $Me_2C(Cp)(Flu)ZrCl_2$ (**III-1**) is evidence that the E–N copolymer chain

migrates to the N coordination site and supports an alternating mechanism. Kaminsky [65] found that E–N copolymerization with the C_s symmetric metallocene **III-1** follows first-order Markov statistics. Our preliminary calculations at tetrad level are in agreement with this observation.

The formation of *meso* NN diads with catalysts **I-2** and **I-5** is dictated by the catalyst symmetry. The experimental tetrad distributions and those calculated according to first- and second-order Markovian models showed that the lower is the tendency to alternate the two comonomers, the stronger is the need for using model M2 to describe the copolymerization statistics. Thus, it is possible to state that the next-to-last E or N monomer unit exerts an influence on the reactivity of the propagating Mt–E* or Mt–N* species. Such an influence seems to be contingent upon the catalyst structure.

At higher norbornene concentrations, probably owing to norbornene coordination, copolymers with all catalysts may need more complex models.

2.7. Living E–N copolymerizations

Living polymerization is one of the most useful tools for the synthesis of polymers with precise control over molecular weight, composition, and architecture, such as block copolymers and terminally functionalized polymers. These controlled polymers are expected to endow materials with unique properties. Quite a few efficient and selective catalysts for the living polymerization of ethene, propene, 1-hexene, or other olefins have recently been developed [66]. Examples of catalysts, less exotic with respect to those required for living olefin copolymerization, that copolymerize E and N in a (quasi) living fashion exist. Cherdron et al. [31] announced the possibility of controlling the reaction conditions to achieve "quasi-living" polymerization and described a shift of the molar mass distribution (MMD) in time for the E–N copolymerization. However, no mention of the catalyst used nor details of experimental conditions were given.

We have found that catalysts such as *rac*-Et(Indenyl)$_2$ZrCl$_2$ (**I-2**), Me$_2$Si(Me$_4$Cp)(N-^{t}Bu)TiCl$_2$ (**IV-1**), *rac*-Et(4,7-Me$_2$indenyl)$_2$ZrCl$_2$ (**I-3**), and 90% *rac*/10% *meso*-H$_2$C(3-^{t}Bu-Indenyl)$_2$ZrCl$_2$ (**I-9**)/MAO under usual conditions, that is, by using MAO freed from AlMe$_3$ and [Al]/[Zr] molar ratios as high as 2000, promote E–N copolymerization with both yield and molar masses growing with time. The molecular mass of E–N copolymers, obtained at low temperatures (T = 30–50 °C) and high norbornene feed fractions, increases with time for up to 1 h. The polydispersity can be as narrow as 1.1 at [N]/[E] feed ratios as high as 28 [66]. This indicates that very little chain transfer occurs and that E–N copolymerizations are quasi-living under these conditions. Chain growth over 1 h is unusual for olefin polymerization, the average lifetime of a growing ethene and propene polymer chain is typically less than seconds, and growth of polymer chain can only be observed with stopped-flow techniques. The type of catalyst used has a strong influence upon the quasi-living character of the reaction.

Two recent reports have appeared on E–N living copolymerization and the synthesis of E- and N-based block copolymers by Li et al. [35] and by Yoshida et al. [34]. They used bis(-enaminoketonato) Ti complexes and bis(pyrrolideimine)Ti complex based catalytic systems, respectively. The latter system also allows the living E polymerization under limited conditions.

The linearity of the growth of molar mass with time allows us to gain insight into the factors influencing the propagation and chain transfer reactions by using standard equations for the treatment of the experimental data of the polymerization kinetics, derived from those introduced by Natta long ago [68].

It was possible to calculate the average turnover frequencies of monomer insertion $\langle f_p \rangle$ and chain transfer or termination $\langle f_t \rangle$ and the [Zr*]/[Zr] values [66] summarized in Table 8.

By comparing the results obtained (Table 8) for catalyst **I-2** at two different N/E ratios, we observe that an increase of the N/E ratio clearly gives a decrease of the monomer insertion turnover frequency. At the same time the transfer turnover frequency decreases so that the ratio $\langle f_t \rangle / \langle f_p \rangle$ remains constant (Table 8). Such a similarity is worth noting since catalysts **I-2** and **I-9** produce completely different polymers: the extremes are **I-2**, a norbornene-rich copolymer at high N concentration, and **I-9**, a virtually pure polyethene over the whole feed composition range.

The results concerning **I-9**, along with its activity, suggest that the decrease in activity has its origin in the complexation of norbornene with the reaction mechanism.

Surprisingly, the values of $\langle f_t \rangle / \langle f_p \rangle$ are very close to those reported by Busico et al. [69] for the stopped-flow homopolymerization of ethene, using *rac*-Me$_2$Si(4-Ph-indenyl)$_2$ZrCl$_2$/MAO, in spite of the difference of several orders of magnitude in absolute values of $\langle f_p \rangle$ and $\langle f_t \rangle$.

The fraction of active sites is higher than the value of 0.1 mol/mol(Zr) reported for ethene polymerization with *rac*-Me$_2$Si(2-methyl-4-phenyl-1-indenyl)$_2$ZrCl$_2$ at very short polymerization time under stopped flow conditions [68]. Under the same conditions the number of active sites found in propene polymerization is six times higher than in ethene polymerization. The values obtained for E–N copolymerization are closer to the values recently counted by Landis (0.85–0.95 mol/mol(Zr)) [70] for the polymerization of 1-hexene with dimethylmetallocene **I-2**. Each Zr* site spends a fraction of time in the Zr–E* or in Zr–N* state. This depends on the norbornene content in the copolymer and on the catalyst structure.

The relatively higher concentration of Zr* active sites found in E–N copolymerization indicates that the Zr* sites that we measure are mainly in the Zr–N* state. The similarities between $\langle f_t \rangle / \langle f_p \rangle$ values found in E–N copolymerization and E polymerization indicate that Zr–E* sites contribute more to chain propagation and chain transfer than the Zr–N* ones. In conclusion, the presence of norbornene both in the polymer chain and in solution plays a crucial role in the livingness of E–N copolymerization due to its steric hindrance

Table 8
Kinetic parameters of the ethane–norbornene copolymerization [67b]

Symmetry	Catalyst	[N]/[E]	N mol% Incorporated	M_w/M_n	$\langle f_p \rangle$ (min^{-1})	$\langle f_t \rangle$ (min^{-1})	$\langle f_t \rangle/\langle f_p \rangle$ ($\times 10^4$)	Zr^*/Zr
C_2	**I-2**	28.4	59	1.16[a]	346	0.062	1.79	0.68
		12.5	52	1.24[a]	634	0.109	1.72	0.66
	I-3	12.5	36	1.18[a]	185	0.032	1.73	0.94
90% rac/10% meso	**I-9**	12.5	0.5	1.44[b]	381	0.076	1.99	0.56

Polymerization conditions: solvent = toluene, [Al]/[Zr] = 2000; $T = 30\,^{\circ}C$, $P_E = 1.013$ bar.
[a] Polydispersity over the first 10 min of reaction.
[b] Polydispersity over the first 20 min of reaction.

and coordinating ability. This causes a great reduction of the propagation and chain transfer rate compared to that in the homopolymerization of α-olefins and makes the Zr^* state more or less "dormant".

This agrees with the observation that the long chain branches decrease with increasing N content in the copolymer, when using a catalyst like $Me_2Si(Me_4Cp)(N^tBu)TiCl_2$ [59] which allows for incorporation of long chain branches in polyethene: chain transfer to the monomer and the formation of the vinyl terminated polymer chain are possible only at Mt–E^* sites (Scheme 3).

This picture agrees with the DFT calculations by Yoshida et al. of relative formation energies on the bis(pyrrolideimine)Ti catalytic system [34]. Their estimates indicated that an N coordinated to Ti–E^* species is more stable than the corresponding E-coordinated species by 8.33 kJ/mol, indicative of dominant N coordination to the Ti center of the E-last-inserted species. Such a coordination (−17.05 kJ/mol) would reduce the electrophilicity of the active species and provide steric hindrance around the active site, which probably reduces all the possible chain transfers (e.g., hydrogen transfer to a reacting monomer, chain transfer to alkyl Al species). Thus, the achievement of the controlled living copolymerization probably results from the stabilization of a Ti–E^* species toward chain transfers and its smooth change to a Ti–N^* species stable towards chain-transfers. However, their observation that E–N copolymerization at 90 °C produced a copolymer with broader molecular mass distribution (M_w/M_n 1.86) and possessing a vinyl end group indicates that the Mt–E^* species of this catalyst also undergoes faster chain transfer than the Mt–N^* species.

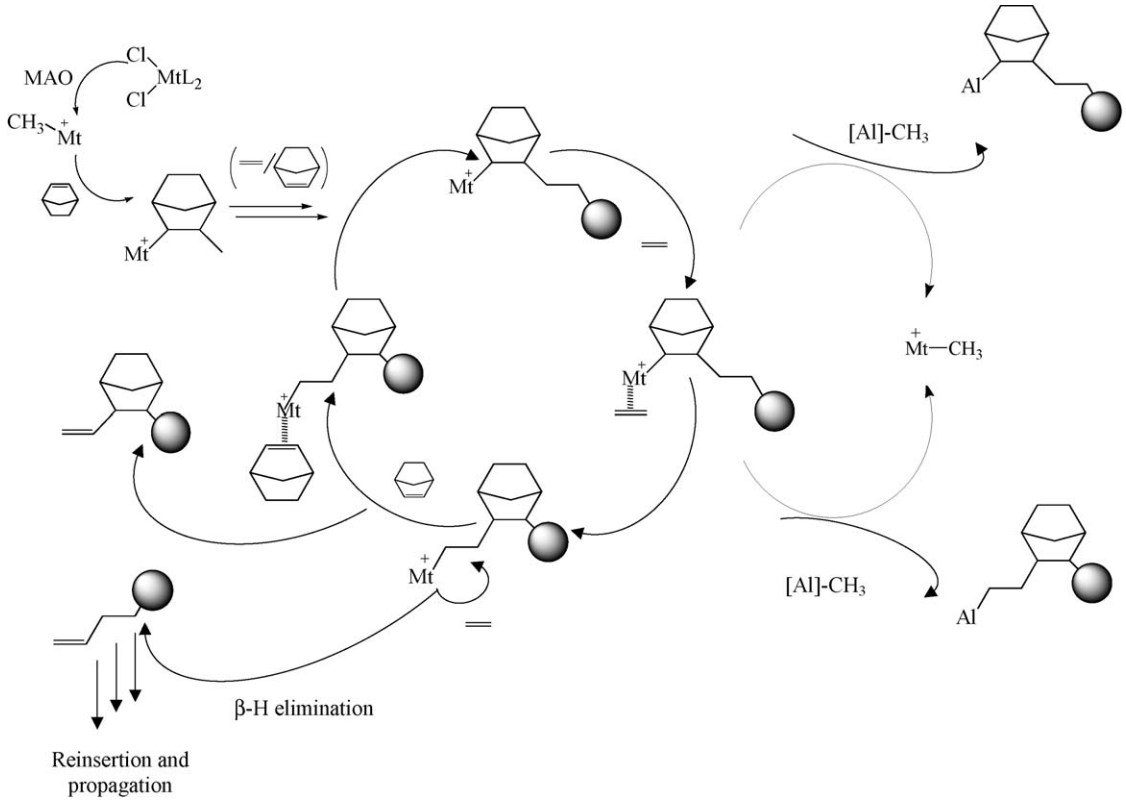

Scheme 3. Mechanism for reaction paths taking part in the catalytic cycle during E–N copolymerization by metallocenes as suggested by Thorshaug et al. [59] implemented with Yoshida's [34] results in living polymerization promoted by **VI**/MAO.

2.8. Chain-end analysis of the E–N copolymers

Studies on copolymerization statistics and copolymer microstructure allow the identification of the factors governing the mechanisms of propagation steps and copolymer tacticity. Information regarding the mechanisms of initiation, termination, and chain-transfer steps is usually achieved by chain-end analysis. In comparison with other ethene or α-olefin polymerizations, chain-growth, termination, and chain-transfer reactions of E–N copolymerizations have not been investigated in similar detail. High molar masses and the possibility of achieving quasi-living polymerizations for some E–N copolymerization systems would make the chain-end analysis rather difficult.

As already explained, chain transfer reactions at a Mt–N bond are rather difficult [71]: the β-H transfer is impossible since it would violate Bredt's rule, that is, the coplanarity of Zr–C(α)–C(β)–H [72]. Chain transfer reactions should occur more often at an E-last inserted-Mt bond.

Yoshida et al. in their study of E–N living copolymerization by bis(pyrrolide-imine) Ti complexes with MAO carried out chain-end analysis of a low molecular weight living copolymer (M_n 1800, M_w/M_n 1.16, N content 50.8 mol%) by ^{13}C NMR spectroscopy [34]. Due to the alternating nature of this copolymer, if the polymerization would start with E insertion into the Ti–CH_3 bond of an initial active species the possible chain-end structures which should be considered for the copolymer are CH_3–E–E–, CH_3–E–N–, CH_3–N–E– for the initiation chain ends and E–E–, E–N–, N–E– for the termination chain ends. However, no signals arising from CH_3–E–E– and CH_3–E–N– chain-ends were detected. A signal at 15.8 ppm assignable to the methyl carbon of the chain-end structure CH_3–N– was observed. Moreover, the signals at 40.6, 41.0, and 45.0 ppm were detected and assigned to C3, C4, and C2 originating from the CH_3–N– chain end, respectively. Thus, the authors concluded that the polymerization by bis(pyrrolide-imine) Ti complexes is initiated by N insertion, which forms the CH_3–N– chain-end structure. This fact is an additional indication of the high incorporation capability of the catalyst system for N.

On the other hand, the terminal chain end structures appeared to be N–E–, since the signals at 29.1, 35.4, 36.8, and 38.6 ppm were detected and assigned to C5, C7, C4, and C3 belonging to the N–E-chain end, respectively. No signals at ca. 12.1 and 12.0–14.0 ppm arising from the CH_3 of E–E– and E–N– were detected. According to the authors these observations indicate that the catalytically active species mostly exists as a Mt–N-last-inserted species during the polymerization time. This is in agreement with our conclusion derived from the number of metal active species calculated from polymerization kinetics [66] and with Choi's results [62] in E–N copolymerization promoted by metallocenes. All these results suggest that, under the conditions employed, the N insertion into the Mt–E species is much faster than the E insertion into the Mt–N species.

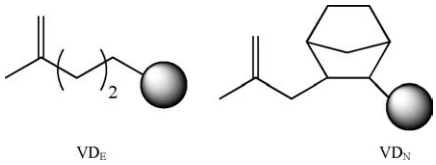

Scheme 4. Unsaturated chain ends observed in E–N copolymers obtained with catalyst Me_2C(Indenyl)(Cp)$ZrCl_2$/MAO [73].

Detailed studies on chain termination and transfer reactions have been carried out in Prof. Brintzinger's group [73]. They were able to detect and identify various types of chain end in E–N copolymerization promoted by Me_2C(Indenyl)(Cp)$ZrCl_2$/MAO (**I-8**) and *rac*-Et(2-^{t}BuMe$_2$SiO-Indenyl)$_2ZrCl_2$/MAO. **I-8** had been selected since it was shown to give rather low molar masses and *rac*-Et(2-^{t}BuMe$_2$SiO-Indenyl)$_2ZrCl_2$ had been observed to give extensive chain transfers to aluminum in ethene polymerization.

In copolymers obtained with catalyst **I-8**/MAO, which contain less than 15 mol% N, the only unsaturated groups present were vinylidene groups, VD_E and VD_N identified by a ^1H NMR signal at 4.8 ppm and by ^{13}C NMR signals at 107.6 and 147.0 ppm (Scheme 4). The authors have assumed that ethylpolymeryl-substituted vinylidene end groups arise via –H transfer after insertion of a 1-butene unit. Indeed, ethyl branches arising from 1-butene insertion have been observed in these copolymers, likely due to dimerization of ethene to 1-butene by this catalyst under the conditions used. Thus, the polymer chain appears to be terminated mainly by a (more facile) –H transfer from the tertiary C atom of one of the rare ethyl branches, rather than from a secondary C atom of the more abundant straight-chain CH_2 groups.

More interestingly, in copolymers with increasing norbornene contents prepared by catalyst **I-8**/MAO and *rac*-Et(2-^{t}BuMe$_2$SiO-Indenyl)$_2ZrCl_2$/MAO, increasing fractions of normal vinylic end groups (^1H NMR multiplets at 5.0 and 5.9 ppm) and norbornenyl end groups (olefinic proton signal at 5.5 ppm) have been detected with comparable intensity. Thus, at higher [N]/[E] feed ratios chain growth appears to be frequently started via vinylic C–H bond activation by norbornene; vinylic end groups could be derived either from vinylic C–H bond activation by ethene or via chain growth termination by –H abstraction from a last-inserted E unit. According to the authors [73], as norbornene incorporation into the copolymer chain approaches its limit, metathetic CH activation under formation of a norbornenyl chain start (Scheme 5) becomes an increasingly prevalent alternative to –H transfer.

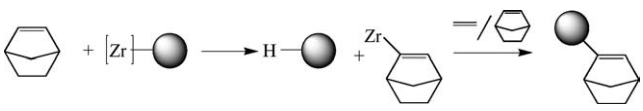

Scheme 5. Norbornenyl chain start from vinylic C–H activation [73].

Addition of aluminum alkyls or zinc alkyls (AlR_3 or ZnR_2, R = Me or Et) to the systems allowed the same authors to study chain transfer reactions from the Zr centers to the aluminum of the cocatalyst. The degree of chain transfer to the cocatalyst should be revealed by the excess of saturated over unsaturated chain end groups. Although it was not possible to quantitatively assess such ratios, studies of catalytic activity and masses of copolymers prepared in the presence of various amounts of AlR_3 or ZnR_2 revealed that chain transfer from copolymers growing at a Zr catalyst center to Al or Zn centers occurs to a considerable extent with both catalysts studied. $Al(iBu)_3$ was found to have an activating effect in polymerization activity and to increase copolymer molar masses. Increased molar masses of copolymers obtained in the presence of added $Al(iBu)_3$ indicated that the AliBu unit has no tendency to exchange iBu group for a polymer chain growing at a Zr center. These observations have also been interpreted in terms of reversible adduct formation between Al or Zn alkyls and cationic zirconocene alkyl species.

2.9. Density functional studies of E–N copolymerization

The above reported systematic experimental studies on metallocene catalysts allowed the identification of factors governing the copolymerization activity, copolymer tacticity, and molar mass, in each catalyst group. Modern density functional calculations can help to understand fundamental issues [74]. Kim and Klein [75] have recently reported DFT studies to address questions such as what dictates the dominance of exo over endo configuration for a norbornene residue in the resulting copolymer and how does a bulky norbornene compete with ethene in the monomer insertion process.

They have performed density functional calculations on simple metallocene ions $Cp_2ZrCH_3^+$ and $H_2Si(CpNH)ZrCH_3^+$, representing metallocene and constrained-geometry catalysts (CGC), respectively. They have established how the sterically hindered norbornene competes with ethene during the insertion. According to these calculations, norbornene is highly reactive at low temperature because the cyclopentyl group helps the insertion providing additional agostic sites and ring strain, instead of hindering the insertion due to steric barriers. This effect becomes more marked on the less sterically hindered catalyst. Steric interaction between the bulky ethene bridge of norbornene and catalysts resulted to unfavor endo-norbornene insertion. The non-reactivity of a structurally similar bicyclooctene seemed to derive from the small geometric difference, which greatly affects the agosticity, steric hindrance, and ring strain of a cycloolefin.

DFT calculations coupled with polymerization behavior have been helpful to Yoshida et al. to understand the origin of living E–N copolymerization by the bis(pyrrolide-imine)Ti complex/MAO system [34]. As referred above, from the analysis of chain-end groups the polymer chain seems to initiate with the formation of the $Ti–N–CH_3$ species. Since this catalyst favors the synthesis of an alternating copolymer, the polymer chain will grow through the insertion of E into the $Ti–N–CH_3$ bond. The DFT calculations of relative formation energies indicated that the N coordination to a $Ti–E^*$ species results to be more stable than the corresponding E-coordinated species by 8.33 kJ/mol. This is indicative of dominant N coordination to the Ti center of the E-last-inserted species. The coordination of highly nucleophilic and sterically encumbered N to the E-last-inserted active species would reduce the electrophilicity of the active species. The N steric encumbrance in the vicinity of the active site would probably limit chain transfers to monomer or to alkyl Al species. Moreover, the N-last-inserted species is quite stable toward chain transfers because of the difficulty in β-H transfers.

In contrast, E-coordination to a $Ti–N^*$ species resulted to be more stable than the corresponding N-coordination by 5.70 kJ/mol, which may result in the formation of the N–E sequence.

Thus, Yoshida et al. [34] concluded that the highly controlled living polymerization by the bis(pyrrolide-imine)Ti complex/MAO system derives from the fact that the catalyst possesses high affinity and high incorporation ability for norbornene due its facile coordination to the $Ti–E^*$ species and its fast insertion as well as from the living character of E polymerization with this catalyst.

Fink et al. performed DFT calculations on $H_2C(Cp)_2$ Zr–NN complexes to model the feasibility of σ-bond metathesis, which explain the observed formation of N tetramers and pentamers, with unusual linkages, by **I-8**/MAO [19]. By means of X-ray crystallography and 2D NMR spectroscopy, norbornene resulted to be connected by *2-exo,2′-exo* linkages except for a *2-exo,7′syn-exo* linkage in the tetramer and pentamers. This structure was hypothesized to derive from σ-bond metathesis occurring after three consecutive N insertions as a result of a conformational change, so that the syn hydrogen at 7′ can interact with Zr. Then the Zr-alkyl undergoes a new *cis*-2,3-*exo* insertion. DFT calculations supported this hypothesis: a γ-agostic conformer initially formed after norbornene insertion can rearrange into a low-energy ε-agostic conformer, suitably oriented for σ-bond metathesis (Scheme 6).

3. Propene–norbornene copolymers

3.1. Synthesis and structure

The incorporation of norbornene into the isotactic polypropene chain was expected to feature higher T_g than E–N copolymers with the same N content and molar mass (MM) since polypropene (PP) has a higher T_g than polyethene [50,49,51,43]. It was to be expected that a detailed interpretation of P–N copolymer spectra could meet greater difficulties than those met in E–N copolymers. Indeed, differ-

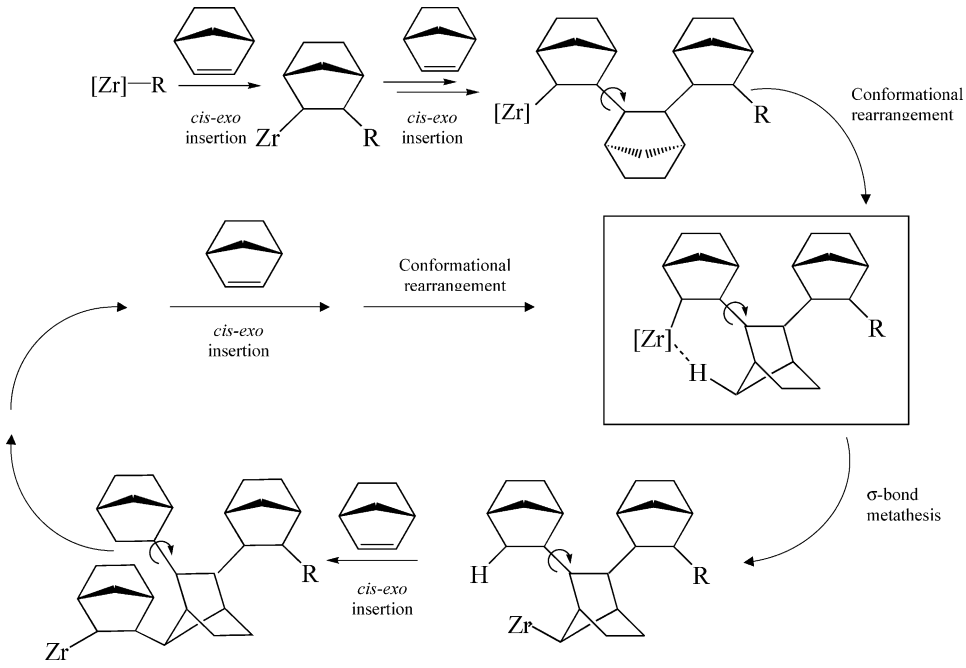

Scheme 6. Mechanism proposed by Fink and co-workers [21] for the combination of *cis*-2,3-exo insertion and α-bond metathesis in N polymerization with catalyst **I-2**.

ences in stereo- and regioregularity of propene units as well as in the comonomer distribution and the stereoregularity of the bicyclic units will originate complex microstructures of the polymer chain and complex spectra. Likely, that is the reason for the limited reports on these copolymers. At the onset of our investigation [28,29] to the best of our knowledge only one article concerning propene–norbornene (P–N) copolymers had been published [76] besides short references to propene-based co- and terpolymers [3].

3.1.1. P–N copolymers with isolated N units

Catalysts **I-2** and **I-4** were selected as *ansa*-metallocenes of C_2 symmetry that have proven effective for producing prevailingly isotactic and regioregular polypropene [78] as well as E–N copolymers with a tendency to alternate [50,26,60]. Catalyst **III-1** was selected as a metallocene of C_s symmetry which yields prevailingly syndiotactic polypropene and is very active in E–N copolymerization.

In Table 9, copolymerization activities and copolymer properties obtained with **I-2**/MAO and **I-4**/MAO, at 30 °C are compared with previous Henschke's results [76] obtained with **I-4**/MMAO at 60 °C. The table shows that as the feed ratio ([N]/[P]) increases the productivity decreases, as expected. The polymerization activities of **I-2** and **I-4** were found to be quite low especially when compared to those obtained for E–N copolymerization under analogous experimental conditions.

This seems to result from the difficulty of inserting a propene into the Mt–tertiary carbon bond formed after the norbornene insertion (Mt–N). Indeed, such a situation is even more sterically crowded than the sites formed after a propene (2,1) region-irregular insertion, which have a lower reactivity with respect to sites with a primary growing polypropene chain [78].

On the basis of the final assignments discussed below it was possible to estimate the molar fractions of norbornene (f_N) and propene (f_P) incorporated in these copolymers. The observation of a great discrepancy between the values of comonomer content obtained from the areas of norbornene signals and those calculated from the propene methyl signals and of the CH_2 peak area confirmed the existence of propene 1,3 mis-insertions in the Mt–N bond.

In contrast to the low polymerization activity, a surprisingly high norbornene incorporation was reported [76] using **I-4**, although to date no NMR spectra nor details of such calculations are published. The very low polymerization activities obtained with **III-1** seems to be indicative of even greater difficulties of insertion of propene into the Mt–N bond of this catalyst than into the Mt–N carbon bond of catalysts **I-2** and **I-4**.

With the help of DEPT spectra and of the signal assignments obtained we could derive a set of equations relating the peak areas to copolymer composition, thus obtaining an N content value which is the most accurate estimate at the present level of assignments.

These results confirm that, in the presence of the catalysts selected, despite the relatively lower polymerization activity, at low norbornene/olefin ratios it is possible to obtain P–N copolymers which are relatively richer in norbornene than the E–N copolymers prepared in similar conditions. It is conceivable that this could arise from the fact that norbornene

Table 9
P–N copolymerization: activities and properties

Symmetry	Catalyst	Activity (kg pol/mol Zr h)	[N]/[P]	N mol% incorporated	T_g	M_w ($\times 10^{-3}$ g/mol)	M_w/M_n	Ref.
C_2	**I-2**[a]	164	0.05	16	19	14.7	2.68	[28]
		107	0.07	25	37	11.1	1.21	[28]
		70	0.10	13	47	–	–	[28]
		56	0.26	35	119	16.6	2.16	[28]
		33	0.67	33	139	45.5	2.23	[28]
		9	1.00	41	129	43.1	2.21	[28]
	I-4[a]	122	0.05	14	26	17.1	3.66	[28]
		53	0.10	21	50	36.8	1.86	[28]
		38	0.25	29	87	17.0	2.2	[28]
		8	0.67	32	108	24.7	1.69	[28]
		4	1.00	n.d.	115	25.6	2.08	[28]
	I-4[b]	320	0.11	11	22.4	7.6	1.8	[76]
		140	0.33	33	83.7	10.5	1.8	[76]
		100	0.67	40	101.2	10.2	1.8	[76]
		60	1.00	56	140.5	5.4	2.9	[76]
		40	2.33	73	173.7	4.9	3.2	[76]
C_s	**IV-5**[c]	900	0.30	17	53	71.9	1.18	[79]
		1575	0.60	36	112	105.4	1.11	[79]
		865	1.13	58	198	157.3	1.14	[79]
		895	2.00	71	249	180.9	1.16	[79]

[a] Polymerization condition: MAO/Zr = 2000, [Zr] = 2×10^{-5} mol/L; P_P = 1.013 bar, T = 30 °C.
[b] Polymerization condition: MAO/Zr = 370, [Zr] = 1.5×10^{-5} mol/L; P_P = 1.013 bar, T = 60 °C.
[c] Polymerization condition: MAO/Ti = 400, [Ti] = 6.67×10^{-4} mol/L; P_P = 1.013 bar, T = 20 °C

competes more easily with propene than with ethene. Under similar polymerization conditions, **III-1** allows for a lower N incorporation than catalysts **I-2** and **I-4**. It is worth noting that the M_w values of the P–N copolymers are quite low in comparison to those of E–N copolymers [76]. In general T_g values are rather low, owing to the low molar mass of the polymer samples, as well as to a significant amount of propene 1,3-misinsertions.

3.1.2. P–N copolymers with norbornene blocks

During the preparation of this review Shiono and coworkers have published a very interesting report on the P–N copolymerization conducted with dimethyl **IV-5** [79]. They had previously reported that this metallocene when activated with Me_3Al-free MAO (dried MAO) yields living propene and norbornene homopolymerization [80,81]. P–N copolymerizations were carried at 20 °C under atmospheric pressure of propene. Dimethylmetallocene **IV-5** was activated by Me_3Al-free methylaluminoxane (dried MAO), modified methylaluminoxane (MMAO), and $Ph_3CB(C_6F_5)_4/Oct_3Al$. The system activated by $Ph_3CB(C_6F_5)_4/Oct_3Al$ was the most active one and yielded the copolymer with the lowest molecular weight and broadest molecular weight distribution. Dried MAO yielded the copolymer with the narrowest polydispersity. The norbornene content in the copolymer was almost proportional to the N/P feed ratio and T_g of the P–N copolymers increased linearly against the norbornene content in the copolymers, from 53 to 249 °C. The copolymer with the highest T_g contained 71 mol% of norbornene.

3.2. Microstructure of propene–norbornene copolymers

3.2.1. P–N copolymers from C_2 symmetric catalysts

Fig. 13 displays the ^{13}C NMR spectrum of a P–N copolymer prepared with **I-2**/MAO, at [N]/[P] feed ratio of 0.26, along with the final signal assignment. The structure and carbon numbering of an isotactic P–N copolymer are sketched in Fig. 14. *Cis*-2,3-*exo* norbornene insertion is considered to occur into the metal–carbon bond as in E–N copolymerization. All propene consecutive monomer units have the methyls in erythro relationships as in an isotactic polypropene chain.

The spectrum in Fig. 13 shows seven groups of signals with comparable areas due to the norbornene carbons in agreement with the lack of symmetry in the norbornene unit

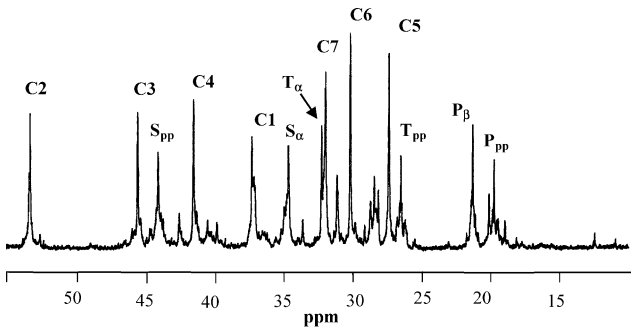

Fig. 13. ^{13}C NMR spectrum of P–N copolymers prepared, at [N]/[P] feed ratio = 0.26, in the presence of **I-2**/MAO.

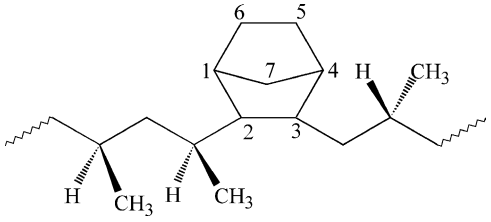

Fig. 14. Structure and carbon numbering of an isotactic P–N copolymer with isolated N units. (Reprinted with permission from Macromolecules 36 (2003) 882–890, Ref. [28].)

of the structure depicted in Fig. 14. DEPT experiments and comparison of the chemical shifts of these signals with those of E–N copolymers allowed us to make a first assignment of the main signals of these copolymers. Ab initio theoretical ^{13}C NMR chemical shifts, combined with RIS statistics of the P–N chain, gave detailed indications [29] for the final ^{13}C NMR assignment for copolymers with N isolated units, shown in Fig. 13 and Table 10.

3.2.2. P–N copolymers from a C_s symmetric catalyst

The spectra of P–N copolymers obtained with **III-1** revealed to be even more complex and showed a multitude of signals with low intensities. A limited assignment of the spectrum has been achieved with the help of DEPT spectra and comparison with chemical shifts of syndiotactic polypropene (s-PP) and with those of P–N obtained with C_2 catalysts [77].

At present the complexity of the spectra of these copolymers prevents from drawing safe conclusions on the tacticity of these copolymers and on regio-regularity of propene insertion in the vicinity of the norbornene unit. However, the limited assignment of the spectra allows us to evaluate the norbornene content and to demonstrate the low tendency of the C_s symmetric **III-1** to give 1,3 propene mis-insertions in P(N copolymers.

3.2.3. P–N copolymers from catalyst $Me_2Si(Flu)(^tBuN)TiMe_2$

The structure of the P–N copolymer produced with catalyst dimethyl **IV-5** was investigated by ^{13}C NMR spectroscopy [79]. The spectra of these P–N copolymers are completely different from those reported above, although they also contain a large number of signals in the same wide

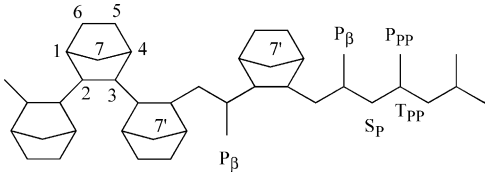

Fig. 15. The structure of a random P–N copolymer with N blocks produced with $Me_2Si(Flu)(^tBuN)TiMe_2$ [81].

range of chemical shifts from 14 to 57 ppm. The authors gave a preliminary assignment with the help of DEPT spectra and comparison with the spectra of polynorbornene and E–N copolymers prepared with the same catalyst [80]. Such an analysis suggested that in these copolymers norbornene units can be connected to the propene unit, that is, isolated or alternating and/or to norbornene in NN dyad sequences. The signals around 50–55 ppm indicated that also longer norbornene sequences are present. Thus, the microstructure of these copolymers is random as shown in Fig. 15.

4. Outlook

Considerable progress in the synthesis of cycloolefin copolymers, in the elucidation of their microstructure, and in the understanding of the copolymerization mechanism has been achieved in these years. Here, for the first time an overview is given of the mechanism for reaction paths taking part in the catalytic cycle in E–N copolymerization in general, and in living norbornene copolymerization in particular, by metal transition catalysts. Nevertheless, there remain some of most challenging areas for further research: (i) the synthesis of catalysts for the incorporation of high norbornene content; (ii) the elucidation of spectra of copolymers with long N blocks and of P–N copolymers; (iii) the reduction of the brittleness of these copolymers when they reach high N content; (iv) the possibility of independently modulating comonomer content, T_g, and molar mass. Promising are the results on E–N and P–N copolymers with high N content and molar masses. Interesting also are the increasing examples of living E–N copolymerization, with a few examples of block copolymers. These block copolymers may have unique properties and be applied to a broad spectrum of appli-

Table 10
Assignments of ^{13}C NMR chemical shifts for carbons of P-N copolymers with N isolated units

Propene			Norbornene		
Carbon	Expected[a] [27]	Observed	Carbon	Expected[a] [27]	Observed
CH_3 (*mmmm*)		18.43–20.43 (19.69)	C5	27.24	27.34
P_β	20.9	21.24	C6	29.79	30.10
CH (*mmmm*)		26.10–26.80 (26.56)	C7	31.98	31.91
T_α		32.30	C1	37.1	37.28
CH_2 (*mmmm*)		43.64–44.69 (44.19)	C4	40.8	41.54
S_α		36.58	C3	43.8/44.3	45.61
			C2	52.5/53.0	53.33

[a] From ab initio and RIS statistical calculations.

cations such as compatibilizers, elastomers, and composite materials.

References

[1] For recent reviews on olefin polymerization, see:
(a) L. Resconi, L. Cavallo, A. Fait, F. Piemontesi, Chem. Rev. 100 (2000) 1253;
(b) G. Coates, Chem. Rev. 100 (2000) 1223;
(c) K. Angermund, G. Fink, Chem. Rev. 100 (2000) 1457;
(d) J. Scheirs, W. Kaminsky (Eds.), Metallocene-based Polyolefins, Wiley, Chichester, 2000;
(e) W. Kaminsky (Ed.), Metalorganic Catalysts for Synthesis and Polymerization: Recent Results by Ziegler–Natta and Metallocene Investigations, Springer-Verlag, Berlin, 1999;
(f) G. Hlatky, Coord. Chem. Rev. 181 (1999) 243;
(g) G.J.P. Britovsek, V.C. Gibson, D.F. Wass, Angew. Chem., Int. Ed. Engl. 38 (1999) 428;
(h) A.L. McKnight, R.M. Waymouth, Chem. Rev. 98 (1998) 2587;
(i) H.H. Brintzinger, D. Fischer, R. Mülhaupt, B. Rieger, R. Waymouth, Angew. Chem., Int. Ed. Engl. 34 (1995) 1143.

[2] G. Sartori, F. Ciampelli, N. Cameli, Chim. Ind. 45 (1963) 1479.

[3] (a) W. Kaminsky, A. Bark, M. Arndt, Makromol. Chem. Macromol. Symp. 47 (1991) 83;
(b) W. Kaminsky, A. Noll, Polym. Bull. 31 (1993) 175;
(c) W. Kaminsky, W. Arndt, Adv. Polym. Sci. 127 (1997) 143;
(d) W. Kaminsky, M. Arndt-Rosenau, in: J. Scheirs, W. Kaminsky (Eds.), Metallocene-based Polyolefins, Wiley, Chichester, 2000, p. 89, and references there;
(e) W. Kaminsky, I. Beulich, M. Arndt, Macromol. Symp. 173 (2001) 211.

[4] (a) N. Calderon, E.A. Ofstead, W.A. Juday, J. Polym. Sci. A-1 (5) (1967) 2209;
(b) N. Calderon, H.Y. Chen, K.W. Scott, Tetrahedron Lett. (1967) 3327;
(c) N. Calderon, E.A. Ofstead, J.P. Ward, W.A. Judy, K.W. Scott, J. Am. Chem. Soc. 90 (1968) 4133;
(d) J.C. Mol, J.A. Moulijn, C.J. Boelhouwer, Chem. Soc., Chem. Commun. (1968) 633;
(e) G. Dall'Asta, D. Motroni, Eur. Polym. J. 7 (1971) 707.

[5] (a) S.W. Benson, F.R. Cruickshank, D.M. Golden, G.R. Haugen, H.E. O'Neal, A.S. Rodgers, R. Shaw, R. Walsh, Chem. Rev. 69 (1969) 279;
(b) P.V.R. Schleyer, J.E. Williams, K.R. Blanchard, J. Am. Chem. Soc. 92 (1970) 2377.

[6] (a) J.M.G. Cowie, Polymers: Chemistry and Physics of Modern Materials, 2nd ed., Chapman & Hall, New York, USA, 1991;
(b) G. Odian, Principles of Polymerization, 3rd ed., Wiley–Interscience, New York, 1991;
(c) J.R. Fried, Polymer Science and Technology, Prentice Hall PTR, Englewood Cliffs, NJ, USA, 1995.

[7] (a) B. Lebedev, N. Smirnova, Macromol. Chem. Phys. 195 (1994) 35;
(b) B. Lebedev, N. Smirnova, Y. Kiparisova, K. Makovetsky, Macromol. Chem. Phys. 193 (1992) 1399;
(c) D. Kranz, M. Beck, Angew. Mackromol. Chem. 27 (1972) 29.

[8] P.A. Patton, C.P. Lillya, T.J. McCarthy, Macromolecules 19 (1986) 1266.

[9] (a) K.J. Ivin, J.C. Mol, Olefin Metathesis and Metathesis Polymerization, Academic Press, San Diego, USA, 1997;
(b) R.H. Grubbs (Ed.), Handbook of Metathesis, vol. 1: Catalyst Development, vol. 2: Applications in Organic Synthesis, vol. 3: Applications in Polymer Synthesis, Wiley–VCH, Weinheim, Germany, 2003.

[10] (a) S. Collins, W.M. Kelly, Macromolecules 25 (1992) 233;
(b) W.M. Kelly, N.J. Taylor, S. Collins, Macromolecules 27 (1994) 4477;
(c) W.M. Kelly, S. Whang, S. Collins, Macromolecules 30 (1997) 3151.

[11] See for example:
(a) P.R. Varanasi, J. Maniscalco, A.M. Mewherter, M.C. Lawson, G. Jordhamo, R.D. Allen, J. Opitz, H. Ito, T.I. Wallow, D. Hofer, L. Langsdorf, S. Jayaraman, R. Vicari, Proc. SPIE-Int. Soc. Opt. Eng. 3678 (1999) 51;
(b) C.G. Wilson, U. Okoroanyanwu, D. Medieros, US Patent 6,103,445 (2000);
(c) P.R. Varanasi, A.M. Mewherter, M.C. Lawson, G. Jordhamo, R. Allen, J. Opitz, H. Ito, T. Wallow, D.J. Hofer, Photopolym. Sci. Technol. 12 (1999) 493.

[12] (a) C. Janiak, P.G. Lassahn, Macromol. Rapid Commun. 22 (2001) 479, A review on the vinyl homopolymerization of norbornene;
(b) A. Sen, T.-W. Lai, Organometallics 1 (1982) 415;
(c) S. Breunig, W. Risse, Makromol. Chem. 193 (1992) 2915;
(d) C. Mehler, W. Risse, Macromolecules 25 (1992) 4226;
(e) A.D. Hennis, J.D. Polley, G.S. Long, A. Sen, D. Yandulov, J. Lipian, G.M. Benedikt, L.F. Rhodes, J. Huffman, Organometallics 20 (2001) 2802;
(f) A.L. Safir, B.M. Novak, Macromolecules 28 (1995) 5396;
(g) A. Abu-Surrah, B.J. Reiger, Mol. Catal. 128 (1998) 239;
(h) B.L. Goodall, L.H. McIntosh III, L.F. Rhodes, Macromol. Symp. 89 (1995) 421;
(i) B.L. Goodall, G.M. Benedikt, L.H. McIntosh III, D.A. Barnes, US Patent 5,468, 819 (1995);
(j) D.A. Barnes, G.M. Benedikt, B.L. Goodall, S.S. Huang, H.A. Kalamarides, S. Lenhard, L.H. McIntosh, K.T. Selvy, R.A. Shick, L.F. Rhodes, Macromolecules 36 (2003) 2623.

[13] M.-J. Brekner, F. Osan, J. Rohrmann, M. Antberg, Process for the preparation of chemically homogeneous cycloolefin copolymers, US Patent 5,324,801 (1994).

[14] Modern Plastics 72 (1995) 137.

[15] R.R. Lamonte, D. Mc Nally, Adv. Mater Process. 3 (2001) 1.

[16] (a) T.R. Younkin, E.F. Connor, J.I. Henderson, S.K. Friedrich, R.H. Grubbs, D.A. Bansleben, Science 287 (2000) 460;
(b) G.M. Benedikt, E. Elce, B.L. Goodall, H.A. Kalamarides, L.H. McIntosh III, L.F. Rhodes, K.T. Selvy, C. Andes, K. Oyler, A. Sen, Macromolecules 35 (2002) 8978;
(c) S.J. Diamanti, P. Ghosh, F. Shimizu, G.C. Bazan, Macromolecules 36 (2003) 9731;
(d) J. Kiesewetter, W. Kaminsky, Chem. Eur. J. 9 (2003) 1750;
(e) S.J. Diamanti, V. Khanna, A. Hotta, D. Yamakawa, F. Shimizu, E.J. Kramer, G.H. Fedrikson, G.C. Bazan, J. Am. Chem. Soc. 126 (2004) 10528.

[17] M. Arndt-Rosenau, I. Beulich, Macromolecules 32 (1999) 7335.

[18] A. Provasoli, D.R. Ferro, L. Boggioni, I. Tritto, Macromolecules 32 (1999) 6697.

[19] M. Arndt, R. Engehausen, W. Kaminsky, K. Zoumis, J. Mol. Catal. A: Chem. 101 (1995) 171.

[20] R.A. Wendt, R. Mynott, K. Hauschild, D. Ruchatz, G. Fink, Macromol. Chem. Phys. 200 (1999) 1340.

[21] C. Karafilidis, H. Hermann, A. Rufińska, B. Gabor, R.J. Mynott, G. Breitensbruch, C. Weidenthaler, J. Rust, W. Joppek, M.S. Brookhart, W. Thiel, G. Fink, Angew. Chem. Int. Ed. 43 (2004) 2444.

[22] M. Arndt, M. Gosmann, Polym. Bull. 41 (1999) 433.

[23] C.H. Bergström, B.R. Sperlich, J. Ruotoistenmäki, J.V. Seppälä, J. Polym. Sci. Part A: Polym. Chem. 36 (1998) 1633.

[24] R.A. Wendt, G. Fink, Macromol. Chem. Phys. 202 (2001) 3490.

[25] (a) A. Provasoli, D.R. Ferro, Macromolecules 10 (1977) 874;
(b) D.R. Ferro, M. Ragazzi, Macromolecules 17 (1984) 485.

[26] I. Tritto, C. Marestin, L. Boggioni, L. Zetta, A. Provasoli, D.R. Ferro, Macromolecules 33 (2000) 8931.

[27] M. Ragazzi, P. Carbone, D.R. Ferro, Int. J. Quantum Chem. 88 (2002) 663.
[28] L. Boggioni, F. Bertini, G. Zannoni, I. Tritto, P. Carbone, M. Ragazzi, D.R. Ferro, Macromolecules 36 (2003) 882.
[29] P. Carbone, M. Ragazzi, I. Tritto, L. Boggioni, D.R. Ferro, Macromolecules 36 (2003) 891.
[30] V. Barone, C. Adamo, J. Chem. Phys. 108 (1998) 664.
[31] H. Cherdron, M.-J. Brekner, F. Osan, Angew. Makromol. Chem. 223 (1994) 121.
[32] A.L. McKnight, R.M. Waymouth, Macromolecules 32 (1999) 2816.
[33] D. Ruchatz, G. Fink, Macromolecules 31 (1999) 4674.
[34] (a) Y. Yoshida, J. Saito, M. Mitani, Y. Takagi, S. Matsui, S. Ishii, T. Nakano, N. Kashiwa, T. Fujita, Chem. Commun. (2002) 1298;
(b) Y. Yoshida, J. Mohri, S. Ishii, M. Mitani, J. Saito, S. Matsui, H. Makio, T. Nakano, H. Tanaka, M. Onda, Y. Yamamoto, A. Mizuno, T. Fujita, J. Am. Chem. Soc. 126 (2004) 12023.
[35] X.F. Li, K. Dai, W.P. Ye, L. Pan, Y.S. Li, Organometallics 23 (2004) 1223.
[36] P. Altamura, A. Grassi, Macromolecules 34 (2001) 9197.
[37] K. Nomura, M. Tsubota, M. Fujiki, Macromolecules 36 (2003) 3797.
[38] M. Arndt, I. Beulich, Macromol. Chem. Phys. 199 (1998) 1221.
[39] (a) N. Herfert, P. Montag, G. Fink, Makromol. Chem. 94 (2001) 3167;
(b) R.A. Wendt, R. Mynott, G. Fink, Macromol. Chem. Phys. 203 (2002) 2531.
[40] B.A. Harrington, D.J. Crowther, J. Mol. Catal. A: Chem. 128 (1998) 79.
[41] W. Kaminsky, P.-D. Tran, R. Werner, Makromol. Symp. 213 (2004) 101.
[42] I. Tritto, L. Boggioni, D.R. Ferro, Macromolecules 37 (2004) 9681.
[43] I. Tritto, C. Marestin, L. Boggioni, M.C. Sacchi, H.H. Brintzinger, D.R. Ferro, Macromolecules 34 (2001) 5770.
[44] D. Ruchatz, G. Fink, Macromolecules 31 (1998) 4674.
[45] R.A. Wendt, G. Fink, J. Mol. Catal. A: Chem. 203 (2003) 101.
[46] M. Arndt-Rosenau, I. Beulich, Macromolecules 32 (1999) 7335.
[47] W. Kaminsky, Macromol. Chem. Phys. 197 (1996) 3945.
[48] (a) B.Y. Lee, Y.H. Kim, Y.C. Won, J.W. Han, W.H. Suh, I.S. Lee, Y.K. Chung, K.H. Song, Organometallics 21 (2002) 1500;
(b) E.S. Cho, U.G. Joung, B.Y. Lee, H. Lee, Y.W. Park, C.H. Lee, D.M. Shin, Organometallics 23 (2004) 4693.
[49] I. Tritto, L. Boggioni, M.C. Sacchi, P. Locatelli, D.R. Ferro, A. Provasoli, in: W. Kaminsky (Ed.), Metalorganic Catalysts for Synthesis and Polymerization, Springer, 1999, p. 493.
[50] I. Tritto, L. Boggioni, M.C. Sacchi, P. Locatelli, D.R. Ferro, A. Provasoli, Macromol. Rapid Commun. 20 (1999) 279.
[51] J. Forsyth, J. Pereña, R. Benavente, E. Perez, I. Tritto, L. Boggioni, H.H. Brintzinger, Macromol. Chem. Phys. 202 (1999) 614.
[52] (a) T. Hasan, T. Shiono, T. Ikeda, Makromol. Symp. 213 (2004) 123;
(b) T. Hasan, T. Shiono, T. Ikeda, Macromolecules 23 (2004) 8503.
[53] G. Odian, Principles of Polymerization, 3rd ed., Wiley, New York, 1991, p. 457.
[54] T. Kelen, F. Tüdos, J. Macromol. Sci.: Chem. A9 (1) (1975) 1.
[55] F.A. Bovey, Polymer Conformation and Configuration, Academic Press, New York, 1969.
[56] K. Soga, T. Uozumi, S. Nakamura, T. Toneri, T. Teranishi, T. Sano, T. Arai, T. Shiono, Macromol. Chem. Phys. 197 (1996) 4237.
[57] W. Kaminsky, R. Engehausen, J. Kopf, Angew. Chem., Int. Ed. Engl. 34 (1995) 2273.
[58] D. Ruchatz, G. Fink, Macromolecules 31 (1998) 4681.
[59] K. Thorshaug, R. Mendichi, I. Tritto, S.C. Trinkle, R. Friedrich, Mülhaupt, Macromolecules 35 (2002) 2903.
[60] I. Tritto, L. Boggioni, J.C. Jansen, K. Thorshaug, M.C. Sacchi, D.R. Ferro, Macromolecules 35 (2002) 616.
[61] M.K. Leclerc, R.M. Waymouth, Angew. Chem. Int. Ed. 37 (1998) 922.
[62] S.Y. Park, K.Y. Choi, K. Ho Song, B.G. Jeong, Macromolecules 36 (2003) 4216.
[63] (a) P. Cossee, Tetrahedron Lett. 12 (1960);
(b) P. Cossee, Tetrahedron Lett. 17 (1960).
[64] For discussion on alternating and retention mechanisms in ethene-propene copolymers with the same catalysts see also:
(a) M.K. Leclerc, R.M. Waymouth, Angew. Chem. Int. Ed. 37 (1998) 922;
(b) W. Fan, M.K. Leclerc, R.M. Waymouth, J. Am. Chem. Soc. 123 (2001) 9555;
(c) M. Arndt, W. Kaminsky, A.-M. Schauwienold, U. Weingarten, Macromol. Chem. Phys. 199 (1998) 1135.
[65] Kaminsky, Private communication.
[66] For a recent review see G.W. Coates, P.D. Hustad, S. Reinartz, Angew. Chem., Int. Ed. (2002).
[67] (a) J.C. Jansen, R. Mendichi, P. Locatelli, I. Tritto, Macromol. Rapid Commun. 22 (2001) 1394;
(b) J.C. Jansen, R. Mendichi, M.C. Sacchi, I. Tritto, Macromol. Chem. Phys. 204 (2003) 522.
[68] G. Natta, I. Pasquon, Adv. Catal. 11 (1959) 1.
[69] V. Busico, R. Cipullo, V. Esposito, Macromol. Rapid. Commun. 20 (1999) 116.
[70] Z. Liu, E. Somsook, C.R. Landis, J. Am. Chem. Soc. 123 (2001) 2915.
[71] D. Ruchatz, G. Fink, Macromolecules 31 (1998) 4684.
[72] P.A. Sykes, Guidebook to Mechanism in Organic Chemistry, 6th ed., Longman Scientific and Technical, Essex, UK, 1986, p. 259.
[73] N. Ni Bhriain, H.H. Brintzinger, D. Ruchatz, G. Fink, Macromolecules 38 (2005) 2056.
[74] See for example:
(a) H. Kawamura-Kuribayashi, N. Koga, K. Morokuma, J. Am. Chem. Soc. 114 (1992) 8687;
(b) T. Yoshida, N. Koga, K. Morokuma, Organometallics 15 (1996) 766;
(c) L. Cavallo, G. Guerra, Macromolecules 29 (1996) 2729;
(d) T.K. Woo, L. Fan, T. Ziegler, Organometallics 13 (1994) 2252;
(e) L. Fan, D. Harrison, T.K. Woo, T. Ziegler, Organometallics 14 (1995) 2018;
(f) P. Margl, J.C.W. Lohrenz, T. Ziegler, P.E. Blöchl, J. Am. Chem. Soc. 118 (1996) 4434.
[75] E.-G. Kim, M.L. Klein, Organometallics 23 (2004) 3319.
[76] O. Henschke, F. Köller, M. Arnold, Makromol. Rapid Commun. 18 (1997) 617.
[77] L. Boggioni, I. Tritto, M. Ragazzi, P. Carbone, D.R. Ferro, Macromol. Symposia 218 (2004) 39.
[78] Y.A. Carvill, I. Tritto, P. Locatelli, M.C. Sacchi, Macromolecules 30 (1997) 7056.
[79] T. Hasan, T. Ikeda, T. Shiono, Macromolecules 38 (2005) 1071.
[80] T. Hasan, A. Ioku, K. Nishii, T. Shiono, T. Ikeda, Macromolecules 34 (2001) 3142.
[81] T. Hasan, K. Nishii, T. Shiono, T. Ikeda, Macromolecules 35 (2002) 8933.